

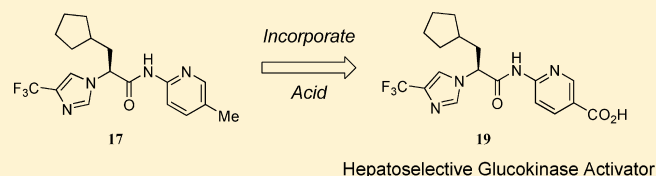
# Discovery of (S)-6-(3-Cyclopentyl-2-(4-(trifluoromethyl)-1H-imidazol-1-yl)propanamido)nicotinic Acid as a Hepatoselective Glucokinase Activator Clinical Candidate for Treating Type 2 Diabetes Mellitus

Jeffrey A. Pfefferkorn,<sup>\*,†</sup> Angel Guzman-Perez,<sup>‡</sup> John Litchfield,<sup>‡</sup> Robert Aiello,<sup>‡</sup> Judith L. Treadway,<sup>‡</sup> John Pettersen,<sup>‡</sup> Martha L. Minich,<sup>‡</sup> Kevin J. Filipowski,<sup>†</sup> Christopher S. Jones,<sup>‡</sup> Meihua Tu,<sup>†</sup> Gary Aspnes,<sup>‡</sup> Hud Risley,<sup>‡</sup> Jianwei Bian,<sup>‡</sup> Benjamin D. Stevens,<sup>†</sup> Patricia Bourassa,<sup>‡</sup> Theresa D'Aquila,<sup>‡</sup> Levenia Baker,<sup>‡</sup> Nicole Barucci,<sup>‡</sup> Alan S. Robertson,<sup>‡</sup> Francis Bourbonais,<sup>‡</sup> David R. Derksen,<sup>‡</sup> Margit MacDougall,<sup>‡</sup> Over Cabrera,<sup>†</sup> Jing Chen,<sup>‡</sup> Amanda Lee Lapworth,<sup>†</sup> James A. Landro,<sup>‡</sup> William J. Zavadowski,<sup>‡</sup> Karen Atkinson,<sup>‡</sup> Nahor Haddish-Berhane,<sup>‡</sup> Beijing Tan,<sup>‡</sup> Lili Yao,<sup>‡</sup> Rachel E. Kosa,<sup>‡</sup> Manthena V. Varma,<sup>‡</sup> Bo Feng,<sup>‡</sup> David B. Duignan,<sup>‡</sup> Ayman El-Kattan,<sup>‡</sup> Sharad Murdande,<sup>‡</sup> Shenping Liu,<sup>‡</sup> Mark Ammirati,<sup>‡</sup> John Knafels,<sup>‡</sup> Paul DaSilva-Jardine,<sup>†</sup> Laurel Sweet,<sup>‡</sup> Spiros Liras,<sup>†</sup> and Timothy P. Rolph<sup>†</sup>

<sup>†</sup>Cambridge Laboratories, Pfizer Worldwide Research & Development, 620 Memorial Drive, Cambridge, Massachusetts 02139, United States

<sup>‡</sup>Groton Laboratories, Pfizer Worldwide Research & Development, Eastern Point Road, Groton, Connecticut 06340, United States

**ABSTRACT:** Glucokinase is a key regulator of glucose homeostasis, and small molecule allosteric activators of this enzyme represent a promising opportunity for the treatment of type 2 diabetes. Systemically acting glucokinase activators (liver and pancreas) have been reported to be efficacious but in many cases present hypoglycaemia risk due to activation of the enzyme at low glucose levels in the pancreas, leading to inappropriately excessive insulin secretion. It was therefore postulated that a liver selective activator may offer effective glycemic control with reduced hypoglycemia risk. Herein, we report structure–activity studies on a carboxylic acid containing series of glucokinase activators with preferential activity in hepatocytes versus pancreatic  $\beta$ -cells. These activators were designed to have low passive permeability thereby minimizing distribution into extrahepatic tissues; concurrently, they were also optimized as substrates for active liver uptake via members of the organic anion transporting polypeptide (OATP) family. These studies lead to the identification of **19** as a potent glucokinase activator with a greater than 50-fold liver-to-pancreas ratio of tissue distribution in rodent and non-rodent species. In preclinical diabetic animals, **19** was found to robustly lower fasting and postprandial glucose with no hypoglycemia, leading to its selection as a clinical development candidate for treating type 2 diabetes.



## INTRODUCTION

Type 2 diabetes mellitus (T2DM) is a rapidly expanding public epidemic affecting over 300 million people worldwide.<sup>1</sup> This disease is characterized by elevated fasting plasma glucose (FPG), insulin resistance, abnormally elevated hepatic glucose production (HGP), and reduced glucose-stimulated insulin secretion (GSIS). Moreover, long-term lack of glycemic control increases risk of complications from neuropathic, microvascular, and macrovascular diseases. The standard of care for T2DM is metformin followed by sulfonylureas, dipeptidyl peptidase-4 (DPP-IV) inhibitors, and thiazolidinediones (TZD) as second line oral therapies.<sup>2</sup> As disease progression continues, patients typically require injectable agents such as glucagon-like peptide-1 (GLP-1) analogues and, ultimately, insulin to help maintain glycemic control.<sup>2</sup> Despite these current therapies, many patients still remain unable to safely achieve and maintain tight glycemic control, placing them at risk of diabetic

complications and highlighting the need for novel therapeutic options.

Among the potential next generation therapies, small molecule glucokinase activators offer a promising opportunity for the treatment of T2DM patients.<sup>3</sup> Glucokinase (GK) converts glucose to glucose 6-phosphate (G-6-P). This enzyme is unique among the members of the hexokinase family given its low substrate affinity ( $K_m \approx 8$  mM), positive substrate cooperativity, and lack of product inhibition.<sup>4</sup> Physiologically, glucokinase functions as a key regulator of glucose homeostasis in the pancreas, liver, and brain. Specifically, in the  $\beta$ -cells of the pancreas, glucokinase acts as a glucostat, establishing the threshold for glucose-stimulated insulin secretion (GSIS).<sup>5</sup> Glucokinase is also expressed in the  $\alpha$ -cells of the pancreas

**Received:** November 4, 2011

**Published:** December 23, 2011

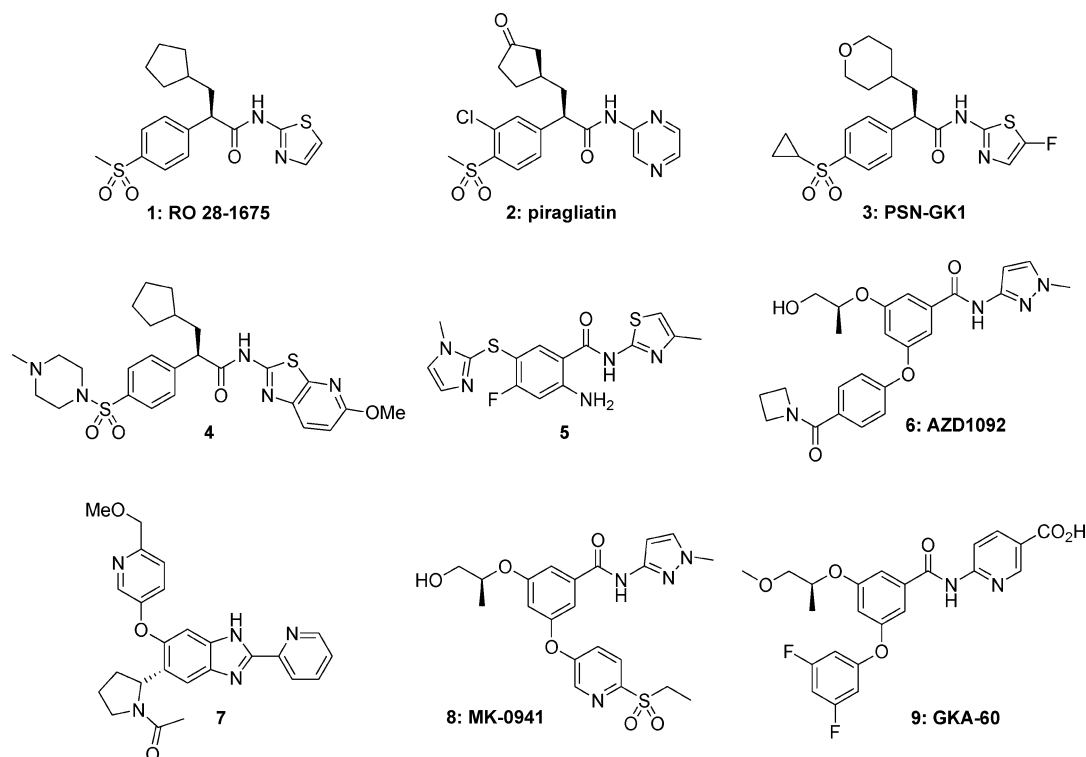


**Figure 1.** Representative structures of glucokinase activators.

where its role is less well characterized but may be involved in regulating glucagon secretion.<sup>6</sup> In hepatocytes, glucokinase represents the rate determining step for hepatic glucose uptake and plays a central role in both glycogen synthesis and the regulation of hepatic glucose production.<sup>7</sup> In the brain, glucokinase is expressed in glucose sensing neurons of the ventromedial hypothalamus where it regulates the counter-regulatory response (CRR) to hypoglycemia.<sup>8</sup> Notably, glucokinase is also found in the endocrine K and L cells of the gut as well as certain pituitary cells where its functions are less well characterized but may be involved in nutrient sensing.<sup>9,10</sup>

Evidence for the importance of glucokinase in regulating glucose metabolism can be found in prominent clinical phenotypes associated with naturally occurring mutations of the enzyme.<sup>11</sup> As an example, heterozygous loss of function mutations are associated with maturity-onset diabetes of the young type 2 (MODY2) while homozygous loss of function mutations are associated with permanent neonatal diabetes. By contrast, human gain of function mutations that activate glucokinase are associated with low blood glucose including hyperinsulinemic hypoglycemia of infancy.

Considering the central role of glucokinase in glucose regulation, there has been significant interest in pharmacological activation of the enzyme as a potential treatment for T2DM. In 2003, Grimsby and co-workers reported the binding of small molecule activators to glucokinase, at an allosteric pocket 20 Å remote from the active site, which influenced the enzyme's kinetic profile by modulating both  $K_m$  for glucose (also known as  $S_{0.5}$ ) and  $V_{max}$ .<sup>12</sup> These efforts resulted in the identification of a phenylacetamide series of activators including clinical candidates **1** and **2** (piragliatin).<sup>12–14</sup> Since this early work, a variety of other structurally diverse glucokinase activators have been reported with representative examples

shown in Figure 1.<sup>15–21</sup> These and other small molecule activators of glucokinase have been recently reviewed.<sup>22</sup>

Consistent with genetic evidence, multiple glucokinase activators have advanced to clinical studies and been shown to lower both fasting and postprandial glucose in healthy subjects and T2DM patients.<sup>23</sup> However, during these same clinical studies, hypoglycemia has been revealed as the key dose limiting adverse effect of glucokinase activators.<sup>23</sup> Several clinical strategies have been employed to manage this hypoglycemia risk including dose titration, dosing with meals, and dosing multiple times a day (b.i.d., t.i.d., etc.) to minimize  $C_{max}$ -driven hypoglycemic events; however, more fundamental changes to the design of activators are perhaps required to resolve this risk and to maximize the therapeutic opportunity of the mechanism.

To overcome the limitations imposed by hypoglycemia risk, several design strategies have emerged to create glucokinase activators with reduced potential for inducing hypoglycemia. As previously reported, one such strategy has been the design of partial activators that avoid reducing glucokinase's glucose  $K_m$  to inappropriately low levels, thereby retaining increased dependence of enzymatic activity on physiological glucose concentrations.<sup>24</sup> A second strategy to mitigate hypoglycemia risk is to restrict enzyme activation to the liver, since the hypoglycemia risk associated with glucokinase activation is postulated to result from potentiation of pancreatic insulin secretion at inappropriately low glucose levels.<sup>16,25</sup> While hypoglycemia risk is mitigated, liver selective activation is still anticipated to offer efficacy given that >99% of the glucokinase enzyme is found in the liver and obese diabetics reportedly lose up to 50% of their hepatic glucokinase activity contributing to reduced hepatic glycogen synthesis and improper regulation of hepatic glucose production (HGP).<sup>26,27</sup> Many diabetic animal models similarly experience loss of hepatic glucokinase activity

with increasing disease severity, and interestingly, normalization of hepatic glucokinase activity via overexpression reduces plasma glucose while also normalizing glycogen levels and restoring regulation of HGP.<sup>28</sup> Additionally, both Bödvarsdóttir<sup>25</sup> and more recently Bebernit<sup>16</sup> (with compound 4, Figure 1) have reported glucose lowering efficacy of liver specific glucokinase activators in preclinical diabetes models. Given the therapeutic opportunity represented by hepatoselective glucokinase activation, herein, we report the discovery of a liver selective development candidate for the treatment of T2DM.

## ■ HEPATOSELECTIVE GLUCOKINASE ACTIVATORS: DESIGN STRATEGY AND SCREENING CASCADE

Since the liver and pancreatic forms of glucokinase are kinetically and enzymatically indistinguishable (differing only in sequence at the extreme amino terminus),<sup>7</sup> we focused on a hepatoselective tissue distribution strategy to achieve selective liver activation. Liver selective drug discovery approaches have been previously reported for various therapeutic classes including HMG-CoA reductase inhibitors,<sup>29</sup> stearyl-CoA desaturase inhibitors,<sup>30</sup> glucocorticoid antagonists,<sup>31</sup> thyroid hormone receptor agonists,<sup>32</sup> hepatitis B and C antivirals,<sup>33</sup> caspase inhibitors,<sup>34</sup> and nucleoside oncolytics.<sup>35</sup> From these examples, a variety of targeting strategies have been used to achieve hepatoselectivity, including (a) optimizing molecules for recognition and active uptake via liver specific transporters such as the organic anion transporting polypeptide (OATP) transporters and organic cation transporters (OCT), (b) synthesizing conjugates with liver targeting motifs such as bile acids or statins, and (c) designing prodrugs that undergo liver specific metabolic activation.<sup>29–35</sup> Among these options we elected to pursue OATP-mediated hepatic uptake given the precedent of preclinical-to-clinical translation with this strategy; consequently, a screening cascade was built to enable parallel optimization of molecules as both glucokinase activators and OATP substrates.

Our testing funnel began with an evaluation of biochemical glucokinase activation where we sought potent activators ( $EC_{50} < 100$  nM) that afforded substantial increases in glucokinase  $V_{max}$  ( $\beta > 1.5$ ) and significant reductions in  $K_m$  ( $\alpha < 0.10$ ). This particular activation profile was targeted as a way to achieve robust enzyme activation and to restore the levels of hepatic glucokinase activity lost during progression of diabetes. The glucokinase activation assay employed recombinant human glucokinase and monitored the rate of glucose 6-phosphate formation using G6PDH/NADP coupling. It was performed in a matrix format wherein dose response determinations for an activator (at 22 different activator concentrations from 0 to 100  $\mu$ M) were conducted at 16 different glucose concentrations (ranging from 0 to 100 mM).<sup>24,36</sup> Analyzing this data using a nonessential activator model enabled determination of an activator's maximum fold effect on reducing the glucokinase  $K_m$  for glucose defined as  $\alpha$  and the maximum fold effect on altering the enzyme's  $V_{max}$  defined as  $\beta$ .<sup>37</sup> Values of  $\alpha$  ranged from 0 to 1 with lower values of  $\alpha$  representing more substantial reductions in the enzyme's glucose  $K_m$ .  $\beta > 1$  represented activator induced increases in the enzyme's  $V_{max}$ . For example,  $\beta = 1.5$  represented a 1.5-fold increase in  $V_{max}$ . Activator potency or  $EC_{50}$  was formally defined as the concentration affording a half-maximal reduction in  $K_m$ .

Concurrent with optimization of biochemical potency we also sought to maximize the therapeutic window against hypoglycemia by achieving enhanced hepatic and impaired

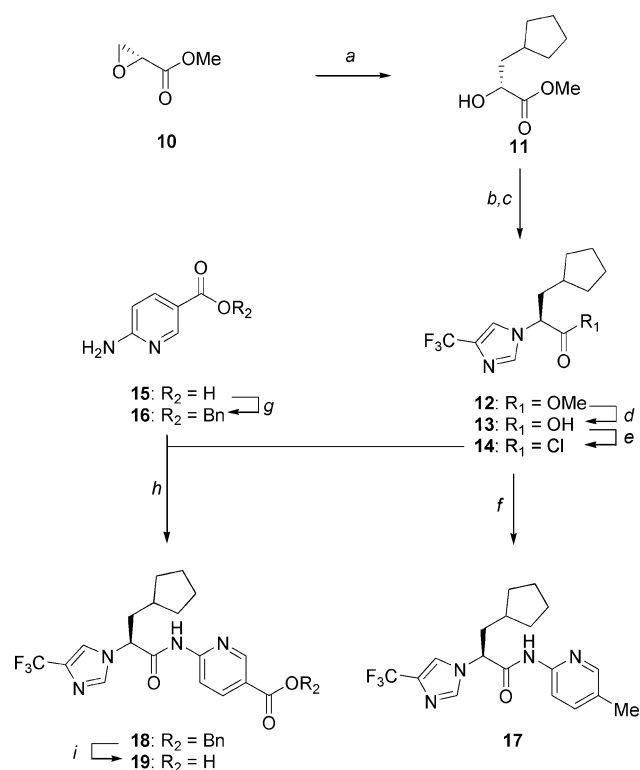
pancreatic tissue distribution. Activators were specifically optimized along three parameters: (a) recognition by liver specific OATP transporters for hepatic uptake, (b) low hepatic oxidative metabolism to maximize residency time and thus pharmacology, and (c) low passive permeability to minimize distribution into peripheral tissues that lack liver specific OATP transporters such as pancreas. Experimentally, evaluation of molecules for OATP-mediated uptake was accomplished using transporter transfected cell lines individually expressing either human or rodent OATP transporters and comparing uptake of analogues between transfected and wild type cells.<sup>38</sup> Oxidative metabolism was evaluated using human liver microsomes. Passive permeability was experimentally evaluated using an RRCK (low efflux MDCK) cell line.<sup>39</sup> Additionally, functional impairment of activators in pancreatic  $\beta$ -cells was evaluated using a rat insulinoma (INS-1) cell line measuring activator effects on glucose stimulated insulin secretion. The ratio of this cellular to rat biochemical potency for a given activator was taken as a surrogate measure of pancreatic impairment with higher values suggesting increased impairment. Analogues that successfully advanced through this screening cascade were then progressed to in vivo pharmacokinetic, tissue distribution, and pharmacology studies.

## ■ SYNTHETIC CHEMISTRY

The synthesis of representative analogues 17 and 19 is illustrated in Scheme 1. Initially, (R)-methyl oxirane-2-carboxylate (10) was added to the in situ generated organocuprate of cyclopentylmagnesium bromide to provide 11 in good yield.<sup>40</sup> Hydroxy ester 11 was then alkylated with inversion of stereochemistry to give 12 using a two-step procedure of triflate formation followed by addition of 4-trifluoromethylimidazole which had been premixed with LiHMDS. The methyl ester of 12 was saponified to the carboxylic acid 13 which was subsequently converted to the corresponding acid chloride 14 under standard conditions. Neutral amides were synthesized by coupling of 14 with appropriate heteroarylamines as illustrated by coupling with 5-methyl-2-aminopyridine to afford 17. Separately, the synthesis of amides bearing acidic moieties was accomplished as illustrated for the preparation of 19 starting from 6-aminonicotinic acid 15 which was first O-benzylated using benzyl bromide and potassium carbonate to yield 16. Coupling of 16 with acid chloride 14 provided the penultimate benzyl-protected 18 that underwent hydrogenolysis over catalytic palladium on carbon to afford 19. By incorporation of alternative heteroarylamines, this route enabled the synthesis of all other analogues investigated in the current studies.

## ■ STRUCTURE–ACTIVITY STUDIES

The starting point for our design efforts was compound 17 (Table 1), which originated from a previous investigation of other *N*-heteroarylacetamides as systemically (i.e., liver and pancreas) acting glucokinase activators.<sup>41</sup> As a lead, activator 17 offered acceptable potency ( $EC_{50} = 114$  nM) and a favorable biochemical activation profile ( $\alpha = 0.04$ ,  $\beta = 1.53$ ); additionally, its relatively low molecular weight (MW = 366) made it amenable to further structural modification. However, 17 was metabolically unstable ( $HLM Cl_{int} > 120$  mL min<sup>-1</sup> kg<sup>-1</sup>), not a substrate for OATP-mediated uptake (Table 1), and exhibited high passive permeability measured in the RRCK assay (17.4  $\times$

**Scheme 1. Synthesis of Representative Glucokinase Activators 17 and 19<sup>a</sup>**

<sup>a</sup>Reagents and conditions: (a) cyclopentylmagnesium bromide, Li<sub>2</sub>CuCl<sub>4</sub>, Et<sub>2</sub>O, THF, -78 → -50 °C, 30 min, 65–70%; (b) Tf<sub>2</sub>O, 2,6-lutidine, CH<sub>2</sub>Cl<sub>2</sub>, 0 °C, 45 min, 100%; (c) 4-trifluoromethylimidazole, LiHMDS, THF, 23 °C, 2 h, 74%; (d) 6 N HCl, 95 °C, 16 h, 98%; (e) (COCl)<sub>2</sub>, cat. DMF, CH<sub>2</sub>Cl<sub>2</sub>, 23 °C, 90 min, 100%; (f) 5-methyl-2-aminopyridine, pyridine, CH<sub>2</sub>Cl<sub>2</sub>, 23 °C, 16 h, 53%; (g) benzyl bromide, K<sub>2</sub>CO<sub>3</sub>, DMF, 23 °C, 16 h, 65%; (h) pyridine, CH<sub>2</sub>Cl<sub>2</sub>, 23 °C, 16 h, 74%; (i) H<sub>2</sub>, 10% Pd/C, ethyl acetate, ethanol, 23 °C, 50 psi, 90 min, 71%.

10<sup>-6</sup> cm/s) and reflected in a 1.3-fold ratio of cellular activity (INS-1) to biochemical potency.

Since acids are a common recognition element of OATP transporters, we envisioned incorporation of a carboxylate into 17 as a strategy to elicit hepatic uptake while concurrently

minimizing passive permeability and oxidative metabolism. To guide installation of the acid, structural biology studies were undertaken to understand the binding of 17 to the allosteric site of human glucokinase. As shown in Figure 2, 17 forms two

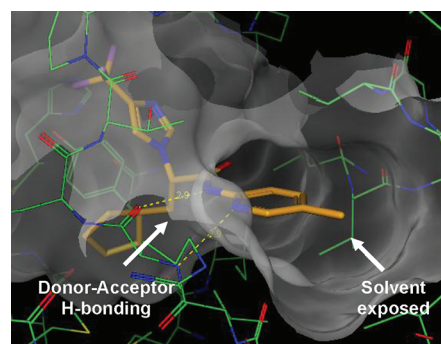


**Figure 2.** Co-crystal structure of 17 bound to the allosteric site of human glucokinase. Crystals of glucokinase in complex of glucose were obtained following published protocols.<sup>17</sup> Cocrystals were obtained by overnight soaking these preformed protein crystals in crystallization mother liquor containing 1 mM 17 before data collection at 17-ID beamline at APS at 100 K, and the structure was determined using the molecular replacement method. Coordinates for this structure have been deposited into the PDB.

hydrogen bonds (donor–acceptor relationship) with the main chain of Arg63. The cyclopentyl group of the activator is located in a hydrophobic pocket formed by side chains of Met210, Ile211, Tyr214, and Met235. Interestingly, the 5-methyl substituent of the 2-aminopyridine is located at a solvent-exposed channel lined with the side chain of Arg63, suggesting that this vector might represent an opportunity to incorporate polar substituents without compromising ligand–protein binding interactions.<sup>42</sup>

To test this hypothesis, the analogue of 17 containing a carboxylate at the 5-position of the 2-aminopyridine ring (19) was synthesized as described previously in Scheme 1. As shown in Table 1, carboxylic acid 19 offered comparable potency and activation profile to its neutral counterpart 17; moreover, 19 exhibited low oxidative metabolism, improved aqueous solubility, and reduced passive permeability. This reduced passive permeability was also reflected by a significant reduction in INS-1 cellular activity (77-fold cell/enzyme ratio versus 1.3-

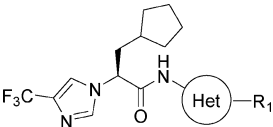
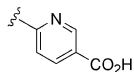
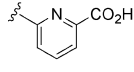
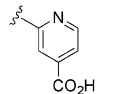
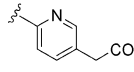
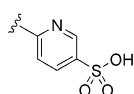
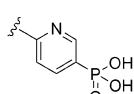
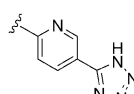
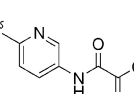
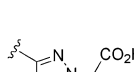
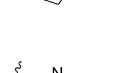
**Table 1. Comparison of Neutral (17) and Carboxylate (19) Containing Glucokinase Activators**

| compd | human GK activation <sup>a</sup> |             |             |  | permeability <sup>b</sup><br>RRCK P <sub>app</sub> (10 <sup>-6</sup> cm/s) | kinetic solubility (μM) | INS-1 cellular activity <sup>c</sup> |                   | transporter substrate <sup>d</sup> |         |
|-------|----------------------------------|-------------|-------------|--|--|-------------------------|--------------------------------------|-------------------|------------------------------------|---------|
|       | EC <sub>50</sub> (nM)            | α           | β           | HLM Cl <sub>int</sub> (mL min <sup>-1</sup> kg <sup>-1</sup> ) |  |                         | EC <sub>50</sub> (nM)                | cell/enzyme ratio | OATP1B1                            | OATP1B3 |
| 17    | 114 ± 41                         | 0.04 ± 0.01 | 1.53 ± 0.08 | >120   | 17.4   | 174                     | 153 ± 0.05                           | 1.3               | no                                 | no      |
| 19    | 90 ± 45                          | 0.03 ± 0.01 | 1.65 ± 0.14 | <8.0   | 1.0  | 524                     | 6900 ± 4090                          | 77                | yes                                | yes     |

<sup>a</sup>Biochemical assay values reported as the arithmetic mean ± SD of *n* > 2 independent determinations. <sup>b</sup>Passive permeability assessed in RRCK canine kidney cell line. <sup>c</sup>Determination of EC<sub>50</sub> for stimulation of insulin secretion in INS-1 cells (rat insulinoma line) at 5 mM glucose. EC<sub>50</sub> values reported as the arithmetic mean ± SD of *n* > 2 independent determinations. Cell/enzyme ratio determined as INS-1 EC<sub>50</sub> divided by the EC<sub>50</sub> of biochemical activation for rat glucokinase enzyme. <sup>d</sup>Human OATP transporters overexpressed in HEK293 cells. Classified as substrate if fold difference in uptake relative to the wild type control is >2.



Table 2. Structure–Activity Relationships for Glucokinase Activators 19–28

|    |    | Human GK Activation <sup>a</sup> |           |           | HLM $Cl_{int}$<br>(ml/min/kg) | Permeability <sup>b</sup><br>RRCK $P_{app}$<br>( $10^{-6}$ cm/sec) | Rat<br>INS-1/Enzyme<br>Ratio <sup>c</sup> | Human<br>OATP1B3 <sup>d</sup> |
|----|---|----------------------------------|-----------|-----------|-------------------------------|--|---|-------------------------------|
|    |   | $EC_{50}$ (nM)                   | $\alpha$  | $\beta$   |                               |  |   |                               |
| 19 |    | 90±45                            | 0.03±0.01 | 1.65±0.14 | <8.0                          | 1.0  | 77  | Substrate                     |
| 20 |    | >10,000                          | ND        | ND        | <8.0                          | 0.7  | ND  | ND                            |
| 21 |    | >10,000                          | ND        | ND        | <8.0                          | ND   | ND  | ND                            |
| 22 |    | 565±61                           | 0.04±0.03 | 1.27±0.14 | <8.0                          | 0.4  | 20  | Substrate                     |
| 23 |    | 2490±1680                        | 0.02±0.01 | 1.63±0.05 | <8.0                          | 0.7  | >10                                       | Substrate                     |
| 24 |   | >10,000                          | ND        | ND        | <8.0                          | 1.1  | ND  | ND                            |
| 25 |  | 284±168                          | 0.04±0.01 | 1.59±0.08 | 160                           | 0.6  | >66                                       | Substrate                     |
| 26 |  | 456±151                          | 0.05±0.01 | 1.30±0.02 | 21.4                          | 0.3  | >100                                      | Substrate                     |
| 27 |  | 1080±353                         | 0.02±0.02 | 1.58±0.07 | <8.0                          | ND   | ND  | ND                            |
| 28 |  | >10,000                          | ND        | ND        | <8.0                          | 1.1  | ND  | ND                            |

<sup>a</sup>Biochemical assay values reported as the arithmetic mean  $\pm$  SD of  $n > 2$  independent determinations. <sup>b</sup>Passive permeability assessed in RRCK canine kidney cell line. <sup>c</sup>Cell/enzyme ratio determined as INS-1  $EC_{50}$  divided by the  $EC_{50}$  of biochemical activation for rat glucokinase enzyme. <sup>d</sup>Human OATP transporters overexpressed in HEK293 cells. Classified as substrate if fold difference in uptake relative to the wild type control is  $>2$ .

fold for parent compound 17). When screened in human OATP1B1 and OATP1B3 transfected cells, 19 was found to be a substrate for both transporters.

Structural variations of 19 were subsequently explored as summarized in Table 2 to further characterize the structure–activity trends in this series. Transposition of the carboxylate from the 5-position of the aminopyridine (19) to either 6-position (20) or 4-position (21) resulted in a significant loss of activity ( $EC_{50} > 10\,000$  nM). Homologation of the carboxylate motif (i.e., 19  $\rightarrow$  22) resulted in 6-fold loss of potency, whereas replacement with either a sulfonic acid (23) or phosphonic acid (24) resulted in more substantial potency losses. Interestingly, conversion of the acid to the tetrazole (25) or oxanilic acid

(26) was reasonably tolerated,  $EC_{50} = 284$  nM and  $EC_{50} = 486$  nM, respectively, and both remained OATP1B3 substrates; however, these isosteres were susceptible to significant oxidative metabolism and thus discontinued. Replacement of the pyridine heterocycle of 19 was also explored examining pyrazole (27) and pyrimidine (28), but these alternative heterocycles were less active. On the basis of these and other supporting structure–activity studies, activator 19 was selected for additional pharmacokinetic and biological profiling given its favorable balance of properties.

## ■ GLUCOKINASE ACTIVATOR 19: PHARMACOKINETICS AND TISSUE DISTRIBUTION

The preclinical protein binding and pharmacokinetic properties of activator **19** are summarized in Tables 3 and 4, respectively.

**Table 3. Plasma and Tissue Protein Binding Properties of Glucokinase Activator 19**

| species | $f_u$               |                    |                       |                    |
|---------|---------------------|--------------------|-----------------------|--------------------|
|         | plasma <sup>a</sup> | liver <sup>b</sup> | pancreas <sup>b</sup> | brain <sup>b</sup> |
| rat     | 0.10                | 0.07               | 0.11                  | 0.09               |
| dog     | 0.17                | 0.09               | 0.21                  | 0.13               |
| monkey  | 0.11                | ND                 | ND                    | ND                 |
| human   | 0.13                | ND                 | ND                    | ND                 |

<sup>a</sup>Plasma protein binding value determined at 50  $\mu$ M using equilibrium dialysis. <sup>b</sup>Tissue protein binding values determined at 1  $\mu$ M using equilibrium dialysis. ND = not determined.

As shown in Table 3, **19** exhibited moderate plasma protein binding ( $f_u = 0.10$ – $0.17$ ) which was consistent across species; additionally, its fraction unbound in tissues of pharmacological interest (i.e., liver, pancreas, and brain) were comparable to fraction unbound in plasma for both rat and dog. Pharmacokinetic studies (Table 4) in rat, dog, and monkey revealed **19** to have high systemic plasma clearance consistent with active hepatic extraction. Evaluation of clearance mechanisms in rat revealed biliary excretion of parent as the primary pathway (62%) with a minor contribution from renal clearance (11%). As suggested by the in vitro microsomal data, in vivo oxidative metabolism of **19** was minimal. In all three preclinical species activator **19** exhibited low to moderate systemic bioavailability (18–35%, Table 4). Subsequent dosing of **19** (5 mg/kg) to portal vein cannulated (PVC) rats revealed a fraction absorbed of 53%. Given that **19** was designed for low passive permeability as a strategy to minimize peripheral distribution, its favorable oral absorption was attributed, in part, to high thermodynamic solubility (4.2 mg/mL at pH 6.5) and a beneficial pH-dependent passive permeability profile as shown in Figure 3. Specifically, under physiological conditions (pH 7.4) **19** has low passive permeability but under more acidic conditions (pH 5.5), which are representative of the upper gastrointestinal tract, carboxylate protonation offers increased passive permeability presumably contributing to oral absorption. Additionally, since **19** was determined to be an OATP substrate (vide infra), active transport may also contribute to its oral bioavailability.

Having characterized the systemic pharmacokinetic properties of **19**, we next sought to characterize its tissue distribution. First, a single oral dose of **19** (50 mg/kg) was administered to Wistar rats followed by sacrifice and determination of free

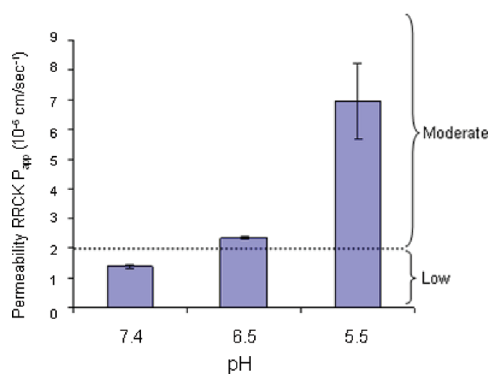


**Figure 3.** pH dependent passive permeability profile of **19**.

plasma, liver, pancreas, and brain drug concentrations of animals at regular intervals ( $t = 0.25, 0.75, 1, 2, 4, 6, 8$ , and 24 h postdose). As shown in Figure 4, **19** exhibited enhanced liver to

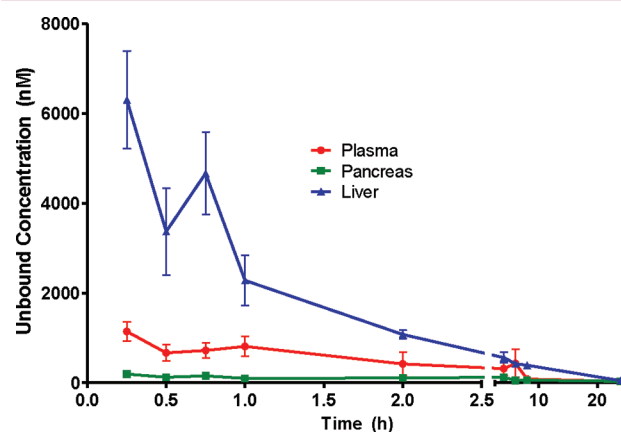


**Figure 4.** Acute tissue distribution time course of **19** in rat after oral administration. Tissue drug concentrations are expressed as the mean  $\pm$  SD ( $n = 3$ ) for free drug concentrations using the fraction unbound values reported in Table 3.

plasma and impaired pancreas to plasma distribution, affording a substantial differential between liver and pancreas exposure. In this same experiment, free brain concentrations of **19** were determined to be exceedingly low and below the limit of quantification at most time points. To further characterize this tissue distribution, repeat dose studies were conducted in both rat and dog, evaluating 28 and 4 days of dosing, respectively. At 4 h postdose on the last day of dosing free drug levels in plasma, liver, pancreas, and brain were determined as summarized in Table 5. Consistent with the observations in the previous acute time course, enhanced liver and impaired

**Table 4. Preclinical Pharmacokinetics of Glucokinase Activator 19<sup>a</sup>**

|           | dose (mg/kg) | AUC <sub>(0–24)</sub> (ng·h/mL) <sup>b</sup> | C <sub>max</sub> (ng/mL) <sup>b</sup> | Cl (mL min <sup>-1</sup> kg <sup>-1</sup> ) | $t_{1/2}$ (h) | Vd <sub>ss</sub> (L/kg) | F (%) |
|-----------|--------------|--|---------------------------------------|---|---------------|-------------------------|-------|
| rat iv    | 1            | 34.7   | 176                                   | 51  | 3.1           | 2.0                     |       |
| rat po    | 5            | 30.3   | 5.4                                   |   |               |                         | 18    |
| dog iv    | 1            | 79.1   | 479                                   | 35  | 2.2           | 1.6                     |       |
| dog po    | 5            | 72.6   | 23.3                                  |   |               |                         | 18    |
| monkey iv | 0.5          | 46.2   | 219                                   | 20  | 1.9           | 0.7                     |       |
| monkey po | 3            | 94.7   | 13.6                                  |   |               |                         | 35    |

<sup>a</sup>Pharmacokinetic parameters expressed as geometric mean of  $n = 2$  animals per group unless otherwise noted. <sup>b</sup>AUC<sub>(0–24)</sub> and C<sub>max</sub> reported as free drug concentrations using the fraction of unbound values reported in Table 3.

Table 5. Tissue Distribution of Activator 19 in Rat and Dog after Repeat Oral Dosing<sup>a</sup>

| species | dose (mg/kg) | treatment duration (days) | ratio        |                 |              |                |
|---------|--------------|---------------------------|--------------|-----------------|--------------|----------------|
|         |              |                           | liver/plasma | pancreas/plasma | brain/plasma | liver/pancreas |
| rat     | 100          | 28                        | 10.5         | 0.14            | BLQ          | 75             |
| dog     | 50           | 4                         | 14.5         | 0.25            | 0.009        | 58             |

<sup>a</sup>Distribution ratios calculated based on free drug concentrations at 4 h postdose on the last day of treatment. BLQ = below limit of quantification.

Table 6. Evaluation of Uptake of Activator 19 into Suspended Rat and Human Hepatocytes

| compd                     | suspended rat hepatocyte uptake rate <sup>a</sup>          |                            | suspended human hepatocyte uptake rate <sup>b</sup>        |                            |
|---------------------------|--|----------------------------|--|----------------------------|
|                           | rate, pmol min <sup>-1</sup> (mg of protein) <sup>-1</sup> | % inhibitable <sup>c</sup> | rate, pmol min <sup>-1</sup> (mg of protein) <sup>-1</sup> | % inhibitable <sup>c</sup> |
| 19                        | 87 ± 21  | 95 ± 5                     | 26   | 93                         |
| rosuvastatin <sup>d</sup> | 218 ± 36   | 96 ± 1                     | 18   | 81                         |
| pravastatin <sup>d</sup>  | 15 ± 3   | 98 ± 3                     | 4.7  | 94                         |

<sup>a</sup>Experiment conducted in freshly isolated rat hepatocytes with data reported as the mean ± SD (*n* = 3 or 4). <sup>b</sup>Experiment conducted in cryopreserved human hepatocytes with data reported from *n* = 1 determination. <sup>c</sup>Inhibition with rifamycin as pan OATP inhibitor. <sup>d</sup>Active control.

Table 7. Evaluation of 19 as a Substrate for Rat and Human Organic Anion Transporters

| compd | rat transporter <sup>a</sup> |         |           | human transporter <sup>a</sup> |           |           |
|-------|------------------------------|---------|-----------|--------------------------------|-----------|-----------|
|       | Oatp1a1                      | Oatp1a4 | Oatp1b2   | OATP1B1                        | OATP1B3   | OATP2B1   |
| 19    | substrate                    | no      | substrate | substrate                      | substrate | substrate |

<sup>a</sup>Conducted in transfected CHO or HEK cells at 1 μM test article. Classified as substrate if fold difference in uptake relative to the wild type control is >2. Active controls were pravastatin (OATP1B1), rosuvastatin (OATP1B3), UK191005 (OATP2B1), pravastatin (Oatp1a1), fexofenadine (Oatp1a4), and estradiol glucuronide (Oatp2b1). Midazolam was used as a negative control in all experiments.

pancreas drug levels (relative to plasma) were observed in both species during these repeat dose experiments with a liver-to-pancreas ratio of 75-fold for rat and 58-fold for dog.

To characterize the active transport mechanism(s) responsible for the selective liver distribution of 19 in rodent and translational relevance to human, we evaluated its uptake into both rat and human suspended hepatocytes (Table 6). In suspended rat hepatocytes, the uptake rate of 19 was greater than pravastatin but less than rosuvastatin; pravastatin and rosuvastatin were used as active controls in the assay. Uptake of 19 was substantially inhibited by rifamycin SV, used as a pan organic anion transporting polypeptide inhibitor. In human hepatocytes, the active uptake rate of 19 was greater than both rosuvastatin and pravastatin and also was significantly inhibited in the presence of rifamycin SV. This significant inhibition of uptake by rifamycin SV in both rat and human hepatocytes indicated the importance of active hepatic uptake and prompted subsequent studies to better understand transporter substrate specificity of 19 in a panel of rat and human organic anion transporting polypeptides as shown in Table 7. Rosuvastatin/pravastatin and midazolam served as positive and negative controls, respectively, in each assay. Compound 19 was found to be a substrate for rat Oatp1a1 and Oatp1b2 transporters but not Oatp1a4; furthermore, 19 was a substrate for human OATP1B1, OATP1B3, and OATP2B1. Taken together, the data from Tables 6 and 7 offered additional confidence that the enhanced liver distribution of 19 observed in rodent and dogs may be relevant to human.

### ■ GLUCOKINASE ACTIVATOR 19: PHARMACOLOGICAL EVALUATION AND COMPARISON TO SYSTEMIC GLUCOKINASE ACTIVATORS

Having identified 19 as a potent glucokinase activator with preferential liver-to-pancreas distribution in preclinical species,

we next undertook more detailed profiling of its biological properties. First, selectivity screening revealed that 19 had no effect on other members of the human hexokinase family (I, II, or III) at concentrations >500-fold its EC<sub>50</sub> for human glucokinase (i.e., hexokinase IV).<sup>43</sup> Additionally, no off-target activity was observed for 19 when evaluated at 10 μM in a broad CEREP screening panel.

In our studies of the functional and pharmacodynamic activity of 19 (vide infra), we included previously reported systemic (i.e., liver and pancreas acting) activators 30 and 31 (Figure 5) as reference compounds to illustrate similarities and

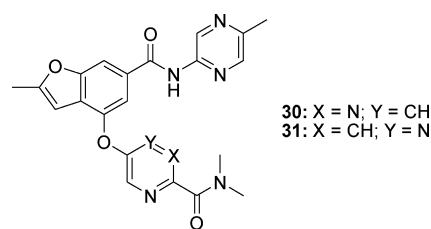
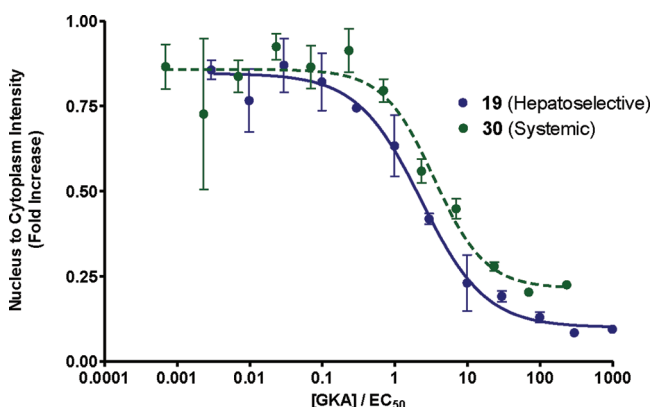


Figure 5. Structures of reference systemic glucokinase activators 30 and 31.

differences between liver specific and systemic glucokinase activation. These two reference compounds were potent (30, EC<sub>50</sub> = 188 nM; 31, EC<sub>50</sub> = 212 nM) activators with high passive permeability (30, RRCK *P*<sub>app</sub> = 20.1 × 10<sup>-6</sup> cm/s; 31, RCK *P*<sub>app</sub> = 22.3 × 10<sup>-6</sup> cm/s) and moderate plasma protein binding (30, rat *f*<sub>u</sub> = 0.24; 31, rat *f*<sub>u</sub> = 0.14).<sup>24</sup> In contrast to the hepatoselective activator, 30 and 31 were not substrates for the OATP transporters and in rodent tissue distribution studies these reference compounds were found to be equally distributed between plasma, liver, and pancreas (ratio of ~1:1:1) with 10-fold brain impairment relative to plasma.<sup>44</sup>

The functional activity of **19** versus the reference systemic activator **30** was first compared using hepatocytes and pancreatic islets. In hepatocytes glucokinase activity is regulated, in part, though an interaction with glucokinase regulatory protein (GKRP).<sup>7</sup> Physiologically, under conditions of low glucose GKRP binds the inactive conformation of glucokinase and sequesters the enzyme to the nucleus. As glucose concentrations increase, glucokinase is released from GKRP and diffuses into the cytoplasm. Given that allosteric glucokinase activators alter the protein conformation, they have been shown to disrupt the GK–GKRP interaction analogous to changes in glucose concentrations, and we therefore characterized the effect of **19** on the subcellular localization of glucokinase in cryopreserved rat hepatocytes. As shown in Figure 6, dose response evaluations of **19** and **30** were



**Figure 6.** Effect of hepatosensitive (**19**) and systemic (**30**) glucokinase activators on glucokinase translocation in cryopreserved rat hepatocytes. Shown is the dose dependent effect of activators **19** and **30** on the translocation of glucokinase from the nucleus to the cytoplasm in cryopreserved rat hepatocytes cultured at 8.9 mM glucose. Data represent the mean  $\pm$  SD ( $n = 3$ ). GKA concentration is normalized by rat  $EC_{50}$  on the X-axis.

conducted in cryopreserved hepatocytes cultured in 8.9 mM glucose and glucokinase translocation from the nucleus to the cytoplasm was monitored via fluorescence based cellomics analysis. Both activators dose-dependently increased glucokinase translocation out of the nucleus with  $EC_{50}$  of 0.19  $\mu$ M for **19** and  $EC_{50}$  of 0.90  $\mu$ M for **30**. As shown in Figure 6, the potency normalized dose response of **19** was left-shifted relative to **30**, consistent with its active hepatic uptake.<sup>45</sup>

In the pancreatic  $\beta$ -cell, glucokinase serves as a glucostat establishing the threshold for glucose-stimulated insulin secretion. Systemically acting glucokinase activators are known to enhance glucose stimulated insulin secretion, so we sought to compare the effects of **19** and **30** on dispersed rat islets in static culture at 11 mM glucose with data reported as percentage of maximum secretion observed at high glucose (22 mM) for INS-1 cells. As shown in Figure 7, reference systemic activator **30** dose-dependently increased glucose-stimulated insulin secretion in these dispersed islets. By contrast hepatosensitive activator **19** demonstrated no significant effect on insulin secretion even at concentrations up to 100-fold its biochemical  $EC_{50}$ , which is consistent with its poor passive permeability.

Having demonstrated the differential functional activity of hepatosensitive activator **19** in isolated hepatocytes versus islets, we then evaluated its activity in whole animal models. In

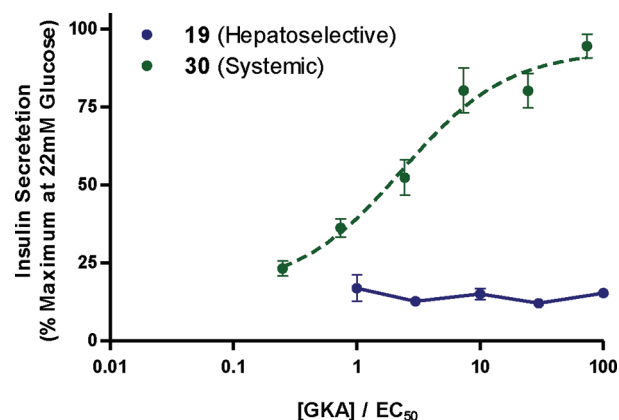


**Figure 7.** Effect of hepatosensitive (**19**) and systemic (**30**) glucokinase activators on insulin secretion in static cultured dispersed rat islets. Shown is the glucose-stimulated insulin secretion in dispersed rat islets in static culture at 11 mM glucose following administration of activator **19** or **30**. Data are expressed as the mean  $\pm$  SD ( $n = 3$ ). GKA concentration is normalized by rat  $EC_{50}$  on the X-axis.

vivo efficacy evaluations were conducted using the Goto–Kakizaki diabetic rat model. Goto–Kakizaki rats spontaneously experience a condition similar to type 2 diabetes mellitus (T2DM) starting at 4 weeks of life which includes (a) basal hyperglycemia (nonfasting plasma glucose range of 180–250 mg/dL), (b) increased hepatic glucose production, and (c) impaired postprandial insulin secretion. An initial study evaluated the effect of **19** versus **31** on reducing fasting plasma glucose after 28-day treatment of Goto–Kakizaki rats at 100 mg/kg. As shown in Figure 8A, the two activators offered comparable efficacy in normalizing fasting plasma glucose at 14 days of treatment and this efficacy was durable through the end of the study. A similar study was then conducted evaluating the effects of both **19** and **31** on fasting plasma glucose levels in normal, nondiabetic Sprague–Dawley rats, as shown in Figure 8B. In contrast to the results in the Goto–Kakizaki diabetic rats, hepatosensitive activator **19** had no effect on fasting plasma glucose; however, systemic activator **31** reduced glucose levels below euglycemia by the first week of treatment. These results are consistent with the hepatosensitive activator correcting the dysregulated hepatic glucose metabolism in the diabetic model while having little effect in normal healthy animals that have intact regulation of hepatic glucose metabolism. The glucose lowering effect of systemic activator **31** in normal, nondiabetic model (i.e., Figure 8B) may be attributed to a leftward shift of the threshold for glucose-stimulated insulin secretion. Notably, this same lack of glucose lowering effect of **19** in normal, euglycemic animals was reproduced in subsequent pharmacology and toxicology (rat, dog, and monkey) studies, increasing confidence in the minimized hypoglycemia risk of this profile relative to that previously observed with systemically acting glucokinase activators.<sup>46</sup>

The effect of hepatosensitive activator **19** on reducing postprandial glucose was also evaluated as illustrated in Figure 9. Activator **19** was again dosed once daily for 28 days (10 and 100 mg/kg) to Goto–Kakizaki rats. A vehicle treated group of Wistar rats was included as a nondiabetic control. An oral glucose tolerance test (OGTT) was performed on day 28 of treatment with **19**, demonstrating a dose-dependent decrease in glucose excursion (Figure 9A) and a 36% decrease in glucose AUC at 100 mg/kg (Figure 9B) with no occurrences of



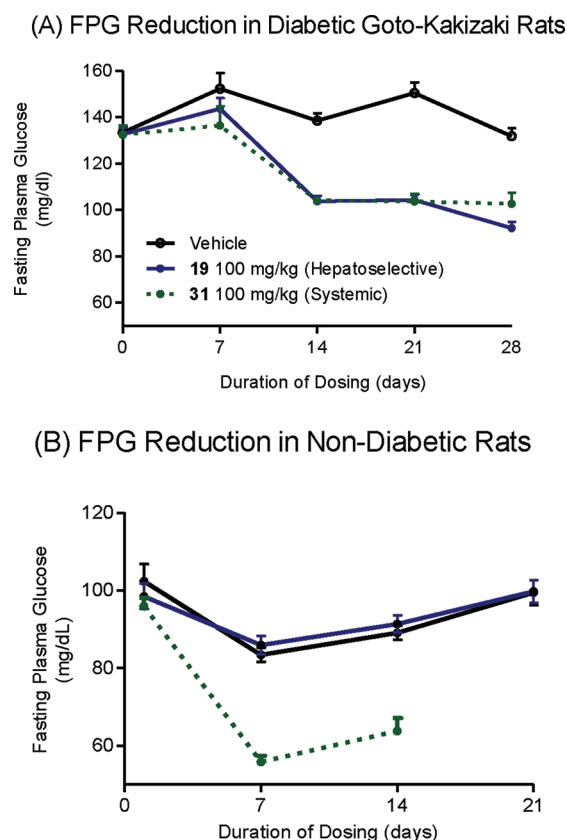


**Figure 8.** Effect of once daily administration of glucokinase activators **19** and **31** on fasting plasma glucose in diabetic (A) and normal, nondiabetic rats (B). (A) Glucokinase activators **19** and **31** were administered orally, once daily for 28 days to Goto–Kakizaki diabetic rats. Weekly fasting glucose samples were collected 1 h postdose, and data are expressed as the mean  $\pm$  standard error ( $n = 8$  per dose group). (B) Glucokinase activators **19** and **31** were administered orally once daily for 21 and 14 days, respectively, to normal, nondiabetic Sprague–Dawley rats. Weekly fasting glucose samples were collected 1 h postdose, and data are expressed as the mean  $\pm$  standard error ( $n = 8$  per dose group).

hypoglycemia. No changes in plasma insulin levels were observed during the course of the OGTT study (Figure 9C). Liver glycogen concentrations were also determined on day 28 for treated animals as shown in Figure 9D. Animals treated with **19** demonstrated a nonstatistically significant trend toward increased liver glycogen, approaching the levels found in normal, nondiabetic animals. This latter observation was in agreement with previous glucokinase overexpression experiments showing the restoration of glycogen synthesis upon increases in hepatic glucokinase activity in diabetic animals.<sup>28</sup> While not shown, a similar OGTT experiment was also conducted in normal, nondiabetic rats undergoing treatment with **19** once-daily for 21 days (10, 30, 100 mg/kg), and results are consistent with the previous fasting glucose observations (i.e., Figure 8B). **19** had no significant effects on reducing postprandial glucose in nondiabetic animals with intact regulation of hepatic glucose metabolism.

The above studies of hepatoselective activator **19** offering glucose lowering efficacy in diabetic animals with dysregulated hepatic glucose uptake and production but not in normal animals illustrate the potential for this approach to normalize hyperglycemia with minimal risk of inducing hypoglycemia. To further characterize its effects on HGP, we also evaluated **19** in

a glucagon challenge experiment as illustrated in Figure 10. In this model, normal (nondiabetic) jugular vein cannulated Wistar rats were administered an iv-glucagon challenge (3  $\mu$ g/kg) to elicit a hyperglycemic glucose excursion via induction of hepatic glycogenolysis.<sup>47</sup> As shown in Figure 10, activator **19**, administered as a single oral dose 50 min prior to challenge, dose-dependently reduced the glucagon-induced glucose excursion, illustrating the strength of glucokinase activation in suppressing glucagon-induced HGP. Since hyperglucagonemia is a key driver of hyperglycemia in T2DM, these glucagon challenge results combined with the efficacy previously observed in Goto–Kakizaki rats (i.e., Figures 7 and 8) highlight the potential for activator **19** to offer significant glycemic reductions in diabetic patients.<sup>48</sup>

In conclusion we have described the design, synthesis, and biological characterization of a hepatoselective glucokinase activator for the treatment of type 2 diabetes. The favorable tissue distribution profile of glucokinase activator **19** coupled with its efficacy and low hypoglycemia risk differentiated it from previous systemic activators, supporting its selection as a development candidate that is currently under clinical evaluation in T2DM patients.

## EXPERIMENTAL SECTION

All reagents and solvents were used as received from commercial sources. <sup>1</sup>H NMR spectra were recorded on a Varian 400 MHz nuclear magnetic resonance spectrometer. <sup>1</sup>H NMR spectra were recorded in CDCl<sub>3</sub>, CD<sub>3</sub>OD, or DMSO-*d*<sub>6</sub>, and chemical shifts are reported relative to the residual solvent peak. The following abbreviations were used to assign spectra: s = singlet, d = doublet, t = triplet, q = quartet, quin = quintet, m = multiplet. Mass spectral analysis was conducted on a Waters Micromass ZQ instrument.

Purity of all final analogues for biological testing were confirmed to be >95% as determined by HPLC analysis. HPLC analysis was conducted according to one of the following methods with the retention time (*t*<sub>R</sub>) expressed in min at UV detection of 254 or 210 nm. For HPLC method A, an Agilent 1100 series HPLC instrument was used, with chromatography performed on an Xbridge 150 mm  $\times$  4.6 mm, 5  $\mu$ m C18 column with mobile phase gradient of 5–100% acetonitrile in water containing 0.1% trifluoroacetic acid and with a flow rate of 1.5 mL/min. For HPLC method B, UPLC was conducted using solvent A consisting of water (0.05% trifluoroacetic acid), solvent B consisting of acetonitrile (0.05% trifluoroacetic acid), and a gradient from 5% to 95%.

Purification was done by either silica gel flash chromatography with a Teledyne Isco CombiFlash Rf with RediSep Flash columns using a gradient of ethyl acetate in heptanes or methanol in CH<sub>2</sub>Cl<sub>2</sub>, or similar instrument or reverse phase preparative HPLC.

For experiments involving the use of animals, all procedures were carried out in compliance with the NIH Guide for the Care and Use of Laboratory Animals under a protocol approved by the Institutional (Pfizer Worldwide Research and Development) Animal Care and Use Committee.

**(R)-Methyl 3-Cyclopentyl-2-hydroxypropanoate (11).** A 0.2 M solution of Li<sub>2</sub>CuCl<sub>4</sub> was prepared as follows: Anhydrous CuCl<sub>2</sub> (26.9 g, 200 mmol) and anhydrous LiCl (17.0 g, 400 mmol) were dissolved in THF (1000 mL). A solution of Li<sub>2</sub>CuCl<sub>4</sub> (0.2 M in THF, 125 mL, 25.0 mmol) was added slowly to a suspension of cyclopentylmagnesium bromide (2 M in diethyl ether, 135 mL, 270 mmol) and THF (500 mL) at  $-50$   $^{\circ}$ C over 2–3 min. The pale gray suspension was then allowed to warm slowly to  $-10$   $^{\circ}$ C over 30 min, by which time the color had developed to a dark gray. The mixture was recooled to  $-78$   $^{\circ}$ C, and (R)-methyl oxirane-2-carboxylate (25.0 g, 245 mmol) was added neat via syringe over 90 s. The mixture was then stirred at  $-78$   $^{\circ}$ C for 20 min, before removing the ice bath and

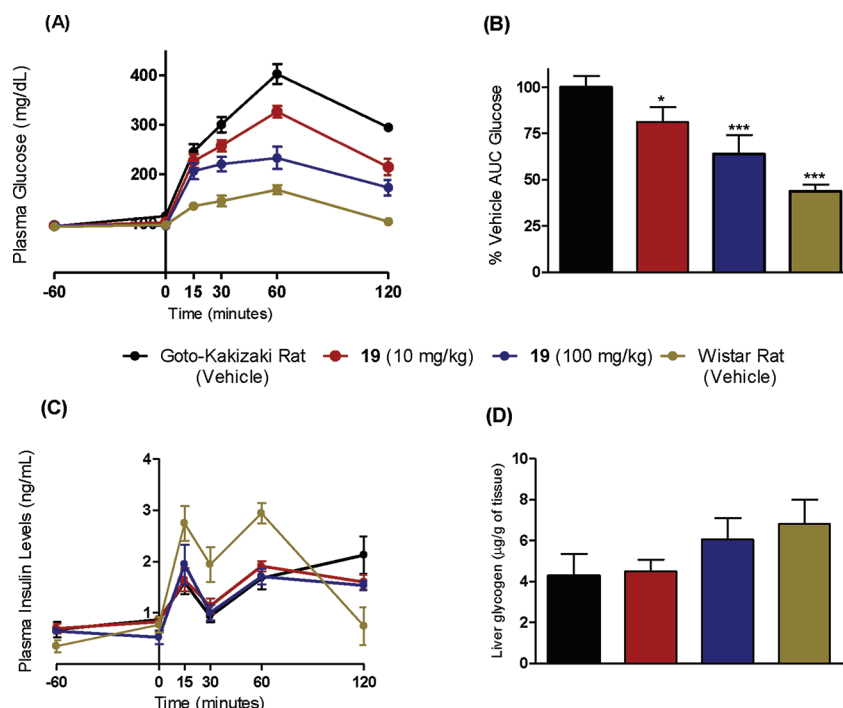


**Figure 9.** Evaluation of in vivo efficacy of activator **19** during an oral glucose tolerance test in diabetic Goto–Kakizaki rats. Glucokinase activator **19** was administered orally once daily (10 and 100 mg/kg) for 28 days to Goto–Kakizaki diabetic rats. (A) Dose dependent effect of **19** on plasma glucose following an oral glucose tolerance test conducted on day 28. Activator was administered at 60 min prior to the administration of a 2 g/kg glucose bolus. Vehicle treated normal, nondiabetic Wistar rats were included for comparison. Data are expressed as the mean  $\pm$  standard error ( $n = 5$  per dose group). (\*  $P < 0.05$ ; (\*\*\*)  $P < 0.001$ ). (B) Effect of **19** on glucose AUC following day 28 oral glucose tolerance test. Data are expressed as the mean  $\pm$  standard error ( $n = 5$  per dose group): (\*  $P < 0.05$ ; (\*\*\*)  $P < 0.001$ ). (C) Effect of **19** on plasma insulin concentrations during an oral glucose tolerance test. Data are expressed as the mean  $\pm$  standard error ( $n = 5$  per dose group). (D) Liver glycogen following 28 days of dosing with **19**. Data are expressed as the mean  $\pm$  standard error ( $n = 4$  per dose group).

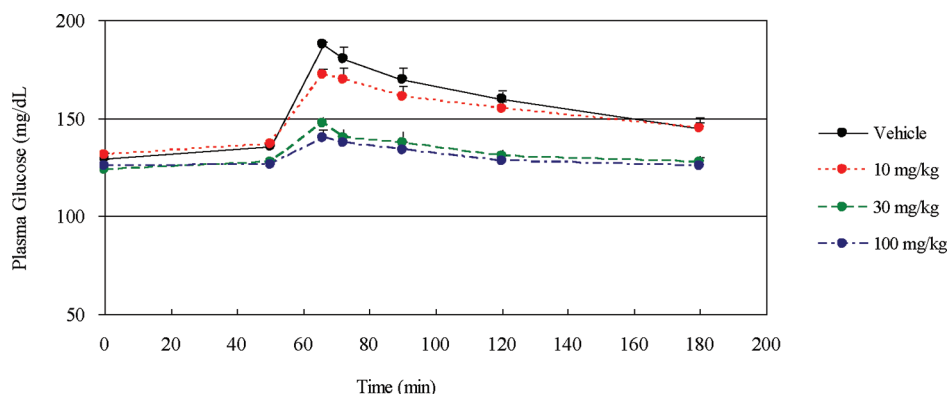


**Figure 10.** Effect of glucokinase activator **19** on plasma glucose during a glucagon challenge in Wistar rats. Wistar rats were dosed orally with **19** (10, 30, 100 mg/kg) at  $t = 0$  min. Glucagon challenge (3  $\mu$ g/kg) was administered iv at  $t = 50$  min. Data are expressed as the mean  $\pm$  standard error ( $n = 6$  per dose group).

allowing the mixture to warm to approximately  $-50^{\circ}\text{C}$  over 30 min. Saturated  $\text{NH}_4\text{Cl}$  (aq, 700 mL) was then added, and the mixture was stirred for 30 min. The organic layer was collected and the aqueous layer extracted with diethyl ether ( $2 \times 250$  mL). The combined organics were washed with saturated  $\text{NH}_4\text{Cl}$  (aq, 350 mL), dried ( $\text{MgSO}_4$ ), and evaporated. Distillation of the crude residue ( $68$ – $70^{\circ}\text{C}$  at 0.8 mbar) afforded **11** as a pale yellow oil (65–70% over multiple batches).  $^1\text{H}$  NMR (400 MHz,  $\text{chloroform-}d$ )  $\delta$  4.16–4.25 (m, 1H), 3.79 (s, 3H), 2.67 (d,  $J = 6.02$  Hz, 1H), 1.95–2.11 (m, 1H), 1.47–1.91 (m, 8H), 1.03–1.21 (m, 2H).

**(S)-Methyl 3-Cyclopentyl-2-(4-(trifluoromethyl)-1H-imidazol-1-yl)propanoate (12).** To a 1 L flask was added **11** (7.29 g, 42 mmol) which was dissolved in anhydrous  $\text{CH}_2\text{Cl}_2$  (300 mL) and placed under nitrogen. The solution was stirred in an ice bath, and 2,6-

lutidine (9.5 g, 88 mmol) was added. A solution of triflic anhydride (20.0 g, 71 mmol) in anhydrous  $\text{CH}_2\text{Cl}_2$  (100 mL) was then added dropwise, and the mixture was stirred for 45 min. The mixture was concentrated, diluted with MTBE, and washed five times with 1 N HCl and once with brine. The organic layer was dried over magnesium sulfate, filtered, evaporated, and dried under high vacuum to afford the crude (R)-methyl 3-cyclopentyl-2-(((trifluoromethyl)sulfonyl)oxy)propanoate (13.0 g, 100%), which was used without further purification.  $^1\text{H}$  NMR (400 MHz,  $\text{chloroform-}d$ )  $\delta$  5.14 (dd,  $J = 3.62, 8.50$  Hz, 1H), 3.85 (s, 3H), 2.04–2.16 (m, 1H), 1.91–2.02 (m, 2H), 1.79–1.90 (m, 2H), 1.50–1.73 (m, 4H), 1.08–1.23 (m, 2H).

4-Trifluoromethylimidazole (3.81 g, 28 mmol) was stirred in anhydrous THF (150 mL) at room temperature under nitrogen. A LiHMDS solution (1.0 M in THF, 25.0 mL, 25.0 mmol) was added

dropwise via addition funnel. After 50 min, a solution of crude (*R*)-methyl 3-cyclopentyl-2-(((trifluoromethyl)sulfonyl)oxy)propanoate (8.52 g, 28 mmol) in dry THF (20 mL) was added. The mixture was stirred for 2 h, then quenched with saturated ammonium chloride. The mixture was diluted with brine and ethyl acetate. The aqueous layer was extracted with ethyl acetate, and the combined organics were dried over sodium sulfate. The mixture was filtered and evaporated to a brown oil. The oil was purified by silica gel chromatography (10% ethyl acetate/heptane gradient to 80% ethyl acetate/heptane) to afford **12** as a clear oil (5.98 g, 74%). <sup>1</sup>H NMR (400 MHz, chloroform-*d*) δ 7.60 (s, 1H), 7.41 (s, 1H), 4.74 (dd, *J* = 6.24, 9.36 Hz, 1H), 3.79 (s, 3H), 2.02–2.19 (m, 2H), 1.45–1.84 (m, 7H), 1.04–1.24 (m, 2H); LCMS *m/z* 290.9 (*M* + *H*)<sup>+</sup>.

**(S)-3-Cyclopentyl-2-(4-(trifluoromethyl)-1H-imidazol-1-yl)propanoic Acid (13).** In a round-bottom flask, **12** (6.61 g, 22.8 mmol) was combined with 6 N HCl (140 mL) and heated to 95 °C for 16 h before cooling. Solid potassium carbonate was added in portions to bring the mixture to pH ~4. Ethyl acetate was added to dissolve the precipitate. The layers were separated, and the aqueous layer was extracted with ethyl acetate. The combined organics were washed with brine, dried over sodium sulfate, filtered, evaporated, and dried under high vacuum to afford **13** as a clear oil (6.15 g, 98%). <sup>1</sup>H NMR (400 MHz, chloroform-*d*) δ 7.84 (s, 1H), 7.41 (s, 1H), 4.76 (dd, *J* = 5.37, 10.05 Hz, 1H), 2.17–2.27 (m, 1H), 2.04–2.15 (m, 1H), 1.45–1.86 (m, 7H), 1.05–1.24 (m, 2H); LCMS *m/z* 277.4 (*M* + *H*)<sup>+</sup>.

**Benzyl 6-Aminonicotinate (16).** To a stirred suspension of 6-aminonicotinic acid (100 g, 0.72 mol) in DMF (700 mL) with brisk mechanical stirring was added K<sub>2</sub>CO<sub>3</sub> (150 g, 1.08 mol). The mixture was stirred for 10 min before the portionwise addition of benzyl bromide (95 mL, 0.80 mol). The mixture was stirred at room temperature overnight. Then the solids were filtered off and washed thoroughly with ethyl acetate. These organics were concentrated under vacuum. The filter cake was dissolved in water and extracted with ethyl acetate. The initial residue after concentration was combined with the ethyl acetate extracts (total volume of 2 L of ethyl acetate). The combined organic extracts were washed with brine (5 × 500 mL), dried (MgSO<sub>4</sub>), and the solvent was removed under reduced pressure. The crude product was refluxed with 1:1 Et<sub>2</sub>O/hexane for 30 min, and then the solids were filtered off (warm), washed with Et<sub>2</sub>O/hexane (1:1), and suction-dried. This solid was precipitated from hot toluene and dried to afford **16** as an off-white solid (107.2 g, 65%). <sup>1</sup>H NMR (400 MHz, chloroform-*d*) δ 8.79 (d, *J* = 1.95 Hz, 1H), 8.05 (dd, *J* = 2.15, 8.59 Hz, 1H), 7.31–7.49 (m, 5H), 6.47 (d, *J* = 8.78 Hz, 1H), 5.34 (s, 2H), 4.91 (br s, 2H); LCMS *m/z* 229.2 (*M* + *H*)<sup>+</sup>.

**(S)-Benzyl 6-(3-Cyclopentyl-2-(4-(trifluoromethyl)-1H-imidazol-1-yl)propanamido)nicotinate (18).** In a round-bottom flask, **13** (6.16 g, 22.3 mmol) was stirred in anhydrous CH<sub>2</sub>Cl<sub>2</sub> (15 mL) at room temperature under nitrogen. Oxalyl chloride (5.8 g, 46 mmol) was added followed by one drop of DMF. After 90 min, the mixture was evaporated and chased twice with 1,2-DCE to afford **14** which was used without additional purification. Amine **16** (5.77 g, 25.3 mmol) was combined with pyridine (3.8 g, 48 mmol) and anhydrous CH<sub>2</sub>Cl<sub>2</sub> (200 mL). This was added to the acid chloride, using another 100 mL of anhydrous CH<sub>2</sub>Cl<sub>2</sub> to aid transfer. The mixture became cloudy. The mixture was stirred for 16 h, then diluted with CH<sub>2</sub>Cl<sub>2</sub> and water. A 1 M solution of potassium dihydrogen phosphate was then added. A solid settled, which was suction-filtered off. The organic layer was extracted with dilute potassium carbonate, washed with brine, dried over sodium sulfate, filtered, and evaporated. The residue was purified by silica gel chromatography (40% ethyl acetate/heptane) to afford **18** as a white solid (8.04 g, 74%). <sup>1</sup>H NMR (400 MHz, DMSO-*d*<sub>6</sub>) δ 11.53 (s, 1H), 8.91 (d, *J* = 1.76 Hz, 1H), 8.34 (dd, *J* = 2.34, 8.78 Hz, 1H), 8.16 (d, *J* = 8.78 Hz, 1H), 7.93–8.01 (m, 2H), 7.45–7.53 (m, 2H), 7.31–7.44 (m, 3H), 5.36 (s, 2H), 5.27 (dd, *J* = 5.27, 10.15 Hz, 1H), 2.15–2.26 (m, 1H), 2.04–2.14 (m, 1H), 1.37–1.71 (m, 7H), 1.27–1.37 (m, 1H), 0.99–1.13 (m, 1H); LCMS *m/z* 487.5 (*M* + *H*)<sup>+</sup>.

**(S)-6-(3-Cyclopentyl-2-(4-(trifluoromethyl)-1H-imidazol-1-yl)propanamido)nicotinic Acid (19).** Intermediate **18** (5.58 g, 11.5 mmol) was divided into two equal portions. Each was dissolved in ethyl acetate (35 mL) and ethanol (70 mL) in a Parr bottle. Then 10%

Pd/C (350–380 mg) was added to each bottle, and the mixtures were shaken under 50 psi hydrogen for 90 min. LCMS showed the reactions to be complete. The mixtures were combined and filtered successively through glass fiber filters until the filtrate was almost clear. The filtrate was concentrated to a smaller volume and run through autovial filters, then evaporated to a glass. Ether was added, and the mixture was stirred for 18 h at room temperature. The resulting white precipitate was filtered, washed with ether, and suction-dried for 20 min. It was then dried under high vacuum at 50 °C for 3 h to afford **19** as a white solid (3.22 g, 71%). <sup>1</sup>H NMR (400 MHz, DMSO-*d*<sub>6</sub>) δ 11.47 (s, 1H), 8.86 (d, *J* = 1.95 Hz, 1H), 8.27 (dd, *J* = 2.24, 8.68 Hz, 1H), 8.13 (d, *J* = 8.78 Hz, 1H), 7.97 (d, *J* = 4.88 Hz, 2H), 5.27 (dd, *J* = 5.37, 9.66 Hz, 1H), 2.04–2.26 (m, 2H), 1.38–1.72 (m, 7H), 1.26–1.37 (m, 1H), 1.08 (td, *J* = 7.88, 11.75 Hz, 1H); LCMS *m/z* 397.5 (*M* + *H*)<sup>+</sup>. HPLC purity (method A): *t*<sub>R</sub> = 7.690 min, 100%.

**(S)-3-Cyclopentyl-N-(5-methylpyridin-2-yl)-2-(4-(trifluoromethyl)-1H-imidazol-1-yl)propanamide (17).** <sup>1</sup>H NMR (400 MHz, chloroform-*d*) δ 8.44 (br s, 1H), 8.11 (br s, 1H), 8.05 (d, *J* = 8.39 Hz, 1H), 7.70 (s, 1H), 7.56 (dd, *J* = 1.85, 8.49 Hz, 1H), 7.53 (s, 1H), 4.71 (t, *J* = 7.51 Hz, 1H), 2.32 (s, 3H), 2.11–2.24 (m, 2H), 1.43–1.85 (m, 7H), 1.13 (td, *J* = 7.90, 11.71 Hz, 2H); LCMS *m/z* 366.9 (*M* + *H*)<sup>+</sup>. HPLC purity (method A): *t*<sub>R</sub> = 7.781 min, 99.49%.

**(S)-6-(3-Cyclopentyl-2-(4-(trifluoromethyl)-1H-imidazol-1-yl)propanamido)picolinic Acid (20).** **20** was prepared according to the method of **19**, substituting commercially available 2-aminopyridine-6-carboxylic acid for 6-aminonicotinic acid. <sup>1</sup>H NMR (500 MHz, DMSO-*d*<sub>6</sub>) δ 11.42 (br s, 1H), 8.24 (d, *J* = 8.29 Hz, 1H), 7.92–8.03 (m, 3H), 7.79 (d, *J* = 7.56 Hz, 1H), 5.28 (br s, 1H), 2.14–2.25 (m, 1H), 2.06–2.14 (m, 1H), 1.37–1.72 (m, 7H), 1.27–1.36 (m, 1H), 1.02–1.15 (m, 1H); LCMS *m/z* 397.1 (*M* + *H*)<sup>+</sup>. HPLC purity (method A): *t*<sub>R</sub> = 7.662 min, 99.50%.

**(S)-2-(3-Cyclopentyl-2-(4-(trifluoromethyl)-1H-imidazol-1-yl)propanamido)isonicotinic Acid (21).** **21** was prepared according to the method of **19**, substituting commercially available 2-aminopyridine-4-carboxylic acid for 6-aminonicotinic acid. <sup>1</sup>H NMR (500 MHz, DMSO-*d*<sub>6</sub>) δ 11.32 (s, 1H), 8.44–8.57 (m, 2H), 7.92–8.03 (m, 2H), 7.56 (d, *J* = 5.86 Hz, 1H), 5.25 (dd, *J* = 5.61, 8.78 Hz, 1H), 2.03–2.25 (m, 2H), 1.37–1.73 (m, 7H), 1.31 (qd, *J* = 7.90, 11.92 Hz, 1H), 1.00–1.14 (m, 1H); LCMS *m/z* 397.1 (*M* + *H*)<sup>+</sup>. HPLC purity (method A): *t*<sub>R</sub> = 7.371 min, 99.30%.

**(S)-2-(6-(3-Cyclopentyl-2-(4-(trifluoromethyl)-1H-imidazol-1-yl)propanamido)pyridin-3-yl)acetic Acid (22).** **22** was prepared according to the method of **19**, substituting 6-aminopyridine-3-acetic acid<sup>49</sup> for 6-aminonicotinic acid. <sup>1</sup>H NMR (400 MHz, DMSO-*d*<sub>6</sub>) δ 12.45 (s, 1H), 11.08 (s, 1H), 8.23 (d, *J* = 1.95 Hz, 1H), 7.90–8.04 (m, 3H), 7.69 (dd, *J* = 2.15, 8.58 Hz, 1H), 5.13–5.32 (m, 1H), 3.60 (s, 2H), 2.02–2.24 (m, 2H), 1.37–1.76 (m, 7H), 1.21–1.35 (m, 1H), 0.99–1.15 (m, 1H); LCMS *m/z* 411.0 (*M* + *H*)<sup>+</sup>. HPLC purity (method A): *t*<sub>R</sub> = 7.552 min, 99.33%.

**(S)-6-(3-Cyclopentyl-2-(4-(trifluoromethyl)-1H-imidazol-1-yl)propanamido)pyridine-3-sulfonic Acid (23).** To a solution of **14** (0.40 g, 1.35 mmol) in dichloromethane (10 mL) were added commercially available 6-aminopyridinesulfonic acid (0.236 g, 1.35 mmol) and pyridine (0.32 mL, 4.1 mmol) at room temperature. The mixture was refluxed for 12 h under a nitrogen atmosphere. The reaction mixture was then concentrated in vacuo and the residue was purified by chromatography on silica to afford **23** (47.2 mg, 8.1%) as a white solid. <sup>1</sup>H NMR (400 MHz, DMSO-*d*<sub>6</sub>) δ 11.18 (s, 1H), 8.50 (s, 1H), 7.98 (m, 4H), 7.03 (s, 1H), 5.22 (m, 1H), 2.18 (m, 2H), 1.60 (m, 4H), 1.48 (m, 3H), 1.31 (m, 1H), 1.11 (m, 1H); LCMS *m/z* 431.4 (*M* – *H*)<sup>–</sup>. HPLC purity (method A): *t*<sub>R</sub> = 6.819 min, 99.72%.

**(S)-6-(3-Cyclopentyl-2-(4-(trifluoromethyl)-1H-imidazol-1-yl)propanamido)pyridin-3-ylphosphonic Acid (24).** To a solution of **14** (0.329 g, 1.12 mmol) in CH<sub>2</sub>Cl<sub>2</sub> (8 mL) was added intermediate 2-aminopyridin-5-ylphosphonic acid ethyl ester<sup>50</sup> (0.257 g, 1.12 mmol) and pyridine (0.265 g, 3.36 mmol) at 25 °C for 12 h. The reaction mixture was concentrated in vacuo and purified by silica gel chromatography (10% petroleum ether/ethyl acetate) to provide intermediate (*S*)-diethyl 6-(3-cyclopentyl-2-(4-(trifluoromethyl)-1H-imidazol-1-yl)propanamido)pyridin-3-ylphosphonate (360 mg, 66.2%)



as a light yellow solid. To a solution of (S)-diethyl 6-(3-cyclopentyl-2-(4-(trifluoromethyl)-1H-imidazol-1-yl)propanamido)pyridin-3-ylphosphonate (170 mg, 0.348 mmol) in  $\text{CH}_2\text{Cl}_2$  (2 mL) was added bromotrimethylsilane (2 mL) at room temperature, and the mixture was stirred for 12 h at 25 °C under a nitrogen atmosphere. The reaction mixture was quenched with methanol (2 mL), and the mixture was concentrated in vacuo. The residue was purified by preparative HPLC [Synergi 150 mm  $\times$  30 mm column, mobile phase from 23% MeOH in water (0.225% formic acid) to 43% MeOH in water (0.225% formic acid)] to afford **24** (47.1 mg, 30.0%) as a white solid.  $^1\text{H}$  NMR (400 MHz,  $\text{CD}_3\text{OD}$ )  $\delta$  8.64 (s, 1H), 8.15 (m, 2H), 7.93 (s, 1H), 7.81 (s, 1H), 5.12 (m, 1H), 2.18 (m, 2H), 1.80 (m, 1H), 1.70 (m, 4H), 1.55 (m, 2H), 1.30 (m, 1H), 1.25 (m, 1H); LCMS  $m/z$  431.4 ( $\text{M} - \text{H}$ ) $^-$ . HPLC purity (method A):  $t_R$  = 6.763 min, 98.74%.

**(S)-N-(5-(2H-Tetrazol-5-yl)pyridin-2-yl)-3-cyclopentyl-2-(4-(trifluoromethyl)-1H-imidazol-1-yl)propanamide (25).** To a solution of **13** (140 mg, 0.31 mmol) in DMF (2 mL) was added benzotriazol-1-yloxytris(dimethylamino)phosphonium hexafluorophosphate (204.6 mg, 0.46 mmol), and the reaction mixture was stirred for 1 h at 25 °C. Subsequently, 5-(1H-tetrazol-5-yl)pyridin-2-amine $^{51}$  (50 mg, 0.31 mmol) and NMM (47 mg, 0.46 mmol) were added. The resulting mixture was stirred at 25 °C for 12 h. The reaction mixture was quenched with saturated aqueous  $\text{NH}_4\text{Cl}$  (1 mL), and the aqueous portion was extracted with EtOAc (20 mL  $\times$  3). The combined organic layers were washed with brine, dried over  $\text{Na}_2\text{SO}_4$ , and evaporated in vacuo. The residue was purified by preparative HPLC [Xbridge 150 mm  $\times$  33 mm column, mobile phase from 6% acetonitrile in water (ammonia added to pH 10) to 26% acetonitrile in water (ammonia added to pH 10)] to afford **25** (10 mg, 10%) as a colorless solid.  $^1\text{H}$  NMR (500 MHz,  $\text{DMSO}-d_6$ )  $\delta$  11.44 (s, 1H), 9.00 (d,  $J$  = 1.95 Hz, 1H), 8.39 (dd,  $J$  = 2.20, 8.78 Hz, 1H), 8.23 (d,  $J$  = 8.54 Hz, 1H), 7.99 (d,  $J$  = 6.34 Hz, 2H), 5.20–5.34 (m, 1H), 2.17–2.26 (m, 1H), 2.08–2.16 (m, 1H), 1.38–1.73 (m, 7H), 1.27–1.37 (m, 1H), 1.02–1.15 (m, 1H); LCMS  $m/z$  421.1 ( $\text{M} + \text{H}$ ) $^+$ . HPLC purity (method A):  $t_R$  = 7.505 min, 99.78%.

**(S)-2-(6-(3-Cyclopentyl-2-(4-(trifluoromethyl)-1H-imidazol-1-yl)propanamido)pyridin-3-ylamino)-2-oxoacetic Acid (26).** To a solution of **14** (2.13 g, 7.2 mmol) in  $\text{CH}_2\text{Cl}_2$  (40 mL) were added 2-amino-5-nitropyridine (1.0 g, 7.2 mmol) and  $\text{Et}_3\text{N}$  (3.12 mL, 21.6 mmol), and the solution was stirred for 12 h at 25 °C under an atmosphere of nitrogen. The reaction mixture was subsequently concentrated under vacuum and filtered through a pad of silica gel to afford intermediate (S)-3-cyclopentyl-N-(5-nitropyridin-2-yl)-2-(4-(trifluoromethyl)-1H-imidazol-1-yl)propanamide (1.1 g, 38.7%) as a light yellow solid. To a solution of (S)-3-cyclopentyl-N-(5-nitropyridin-2-yl)-2-(4-(trifluoromethyl)-1H-imidazol-1-yl)propanamide (0.62 mg, 1.56 mmol) in DMF (20 mL) were added zinc (1.02 g, 15.6 mmol) and a solution of  $\text{FeCl}_3$  (2.53 mg, 15.6 mmol) in water (20 mL) at 25 °C. The resulting mixture was heated to 100 °C with stirring for 3 h. Subsequently, the reaction mixture was cooled, filtered and the filtrate was concentrated under vacuum. Water (20 mL) was added to the resulting residue, and the mixture was extracted with EtOAc (20 mL  $\times$  3). The combined organic layers were washed with brine, dried over  $\text{Na}_2\text{SO}_4$ , and concentrated to afford (S)-N-(5-aminopyridin-2-yl)-3-cyclopentyl-2-(4-(trifluoromethyl)-1H-imidazol-1-yl)propanamide (0.58 g, ~100%) as a light yellow solid that was used without purification.

To a solution of intermediate (S)-N-(5-aminopyridin-2-yl)-3-cyclopentyl-2-(4-(trifluoromethyl)-1H-imidazol-1-yl)propanamide (0.35 g, 0.95 mmol) in  $\text{CH}_2\text{Cl}_2$  (20 mL) were added ethyl chlorooxoacetate (130 mg, 0.95 mmol) and  $\text{Et}_3\text{N}$  (0.41 mL, 2.85 mmol), and the reaction mixture was stirred for 12 h at 25 °C. The reaction mixture was concentrated and the residue filtered through a silica pad to afford (S)-ethyl 2-(6-(3-cyclopentyl-2-(4-(trifluoromethyl)-1H-imidazol-1-yl)propanamido)pyridin-3-ylamino)-2-oxoacetate (130 mg) to which were subsequently added LiI (369 mg, 2.78 mmol) and EtOAc (10 mL). This reaction mixture was heated to reflux for 24 h. The reaction mixture was concentrated under vacuum, and the residue was purified by preparative HPLC [Synergi 150 mm  $\times$  33 mm column, mobile phase from 30% MeOH in water (0.225% formic acid)

to 50% MeOH in water (0.225% formic acid)] to afford **26** (119.1 mg, 45.3%) as a white solid.  $^1\text{H}$  NMR (500 MHz,  $\text{DMSO}-d_6$ )  $\delta$  11.10 (s, 1H), 10.88 (s, 1H), 8.74 (d,  $J$  = 1.71 Hz, 1H), 8.12 (dd,  $J$  = 1.95, 9.03 Hz, 1H), 8.01 (d,  $J$  = 8.78 Hz, 1H), 7.96 (d,  $J$  = 8.54 Hz, 2H), 5.14–5.27 (m, 1H), 2.02–2.24 (m, 2H), 1.36–1.72 (m, 7H), 1.23–1.35 (m, 1H), 1.01–1.15 (m, 1H); LCMS  $m/z$  440.2 ( $\text{M} + \text{H}$ ) $^+$ . HPLC purity (method A):  $t_R$  = 7.522 min, 97.15%.

**5)-2-(3-(3-Cyclopentyl-2-(4-(trifluoromethyl)-1H-imidazol-1-yl)propanamido)-1H-pyrazol-1-yl)acetic Acid (27).** Carboxylic acid **13** (145 mg, 0.525 mmol) was dissolved in dry  $\text{CH}_2\text{Cl}_2$  (5 mL) and stirred at room temperature under nitrogen. One drop of DMF was added, followed by oxalyl chloride (0.095 mL, 1.1 mmol). After bubbling had subsided, the mixture was left stirring for 90 min and then evaporated. The residue was dissolved in two successive portions of 1,2-dichloroethane and evaporated to remove excess oxalyl chloride, and the residue was dissolved in dry  $\text{CH}_2\text{Cl}_2$  (4 mL) to afford **14** which was used without additional purification. Commercially available ethyl 2-(3-amino-1H-pyrazol-1-yl)acetate hydrochloride (130 mg, 0.630 mmol) and pyridine (0.130 mL, 1.61 mmol) were dissolved in dry  $\text{CH}_2\text{Cl}_2$  (5 mL) and added to the  $\text{CH}_2\text{Cl}_2$  (5 mL) solution of acid chloride **14**. The mixture was stirred at room temperature under nitrogen for 24 h. The mixture was then diluted with  $\text{CH}_2\text{Cl}_2$  and water, and the organic layer was separated, washed with brine, dried over sodium sulfate, filtered, and evaporated. The residue was purified by silica gel chromatography (50% ethyl acetate/heptane, linear gradient to 75% ethyl acetate) to afford intermediate (S)-ethyl 2-(3-(3-cyclopentyl-2-(4-(trifluoromethyl)-1H-imidazol-1-yl)propanamido)-1H-pyrazol-1-yl)acetate (153 mg, 68%) which was then combined with lithium hydroxide (50.6 mg, 1.18 mmol) in THF/MeOH/water (1:1:1, 3 mL) and stirred at 25 °C for 2 h. The reaction mixture was then concentrated, and water and 1 N HCl were added to achieve approximately pH 4. A thick precipitate settled. Ethyl acetate was added, and the organic layer was washed with brine and dried over sodium sulfate. The precipitate was filtered, washed, and dried under high vacuum to afford **27** (31.5 mg, 22%).  $^1\text{H}$  NMR (400 MHz, methanol- $d_4$ )  $\delta$  7.93 (s, 1H), 7.80 (s, 1H), 7.54 (br s, 1H), 6.58 (br s, 1H), 5.04 (t,  $J$  = 7.62 Hz, 1H), 4.83 (s, 2H), 2.17 (t,  $J$  = 7.33 Hz, 2H), 1.43–1.89 (m, 7H), 1.21–1.36 (m, 1H), 1.07–1.20 (m, 1H); LCMS  $m/z$  399.9 ( $\text{M} + \text{H}$ ) $^+$ . HPLC purity (method B):  $t_R$  = 0.61 min, 100%.

**(S)-5-(3-Cyclopentyl-2-(4-(trifluoromethyl)-1H-imidazol-1-yl)propanamido)pyrazine-2-carboxylic Acid (28).** **28** was prepared according to the method of **19**, substituting commercially available 5-amino-2-pyrazinecarboxylic acid for 6-aminonicotinic acid.  $^1\text{H}$  NMR (400 MHz,  $\text{DMSO}-d_6$ )  $\delta$  11.79 (s, 1H), 9.36 (s, 1H), 8.98 (s, 1H), 8.00 (s, 2H), 5.30 (dd,  $J$  = 4.59, 10.26 Hz, 1H), 2.18–2.31 (m, 1H), 2.04–2.16 (m, 1H), 1.27–1.75 (m, 8H), 0.97–1.14 (m, 1H); LCMS  $m/z$  398.3 ( $\text{M} + \text{H}$ ) $^+$ . HPLC purity (method B):  $t_R$  = 0.60 min, 99%.

**Method for Determination of Activator Effects on GK Translocation in Cryopreserved Rat Hepatocytes.** Rat primary hepatocytes were obtained from Xenotech (Lenexa, KS) and isolated using its isolation kit following their instructions. The cells were plated into collagen coated 96-well plate with a cell density of 60 000 cells per well in 100  $\mu\text{L}$  per well of high glucose DMEM supplemented with 10% FBS, 100 nM insulin, 10 nM dexamethasone, and 2 mM sodium pyruvate. The plates were incubated in a humidified incubator at 37 °C, 10%  $\text{CO}_2$ . After 4 h, the medium was changed into fresh medium with Matrigel. The plates were incubated overnight. On day 2, cells were changed into DMEM (no glucose) with 10% FBS, 100 nM insulin, 10 nM dexamethasone, 2 mM L-glutamine and incubated overnight. On day 3, the medium was aspirated and an amount of 90  $\mu\text{L}$  of testing glucose medium (8.9 mM glucose DMEM with 0.07% BSA, 1 nM insulin, 10 nM dexamethasone) was added to the plate. Test compounds were serially diluted in DMSO at 1000 $\times$ . Compounds at 10 $\times$  of the final concentrations were diluted in the indicated glucose medium, and an amount of 10  $\mu\text{L}$  per well of these solutions was added to the cell plate. Cells were incubated for 1 h at 37 °C, 5%  $\text{CO}_2$ . Cells in the plates were fixed by adding 100  $\mu\text{L}$  per well of 8% paraformaldehyde for 15 min and followed by 4% paraformaldehyde for 30 min at 4 °C. Plates were then washed 6 times with 300  $\mu\text{L}$  of



PBS per well per cycle using a Bio-Tek ELx 405 microplate washer (Bio-Tek Instruments; Winooski, VT). After the last washing step, the cells were permeabilized using 0.1% TritonX-100 in PBS for 20 min at room temperature. The plates were washed again 6 times with 100  $\mu$ L of PBS per well per cycle. The cells were then blocked by adding 50  $\mu$ L per well of blocking solution (3% BSA, 1% goat serum in PBS) and incubated at room temperature for 1 h. Primary antibody solution (anti-glucokinase antibody diluted 1:250 in blocking buffer) was added to the cells and incubated at 4 °C overnight. The plates were then washed 6 times with 300  $\mu$ L per well per cycle. Secondary antibody solution (AF594-conjugated goat anti-rabbit antibody 1:500 and 2  $\mu$ M Hoechst in PBS) was added to the cells and incubated at room temperature for 1 h. The plate was washed 6 times with 300  $\mu$ L per well per cycle before it was imaged in the ArrayScan (Cellomics). Using GraphPad Prism, version 4.0, dose–response curves were fitted to the following equation:

$$f(x) = \text{low} + 1 + (\text{high} - \text{low}) / [10(\log \text{EC}_{50} - x) \times \text{Hill}]$$

where  $x$  is the concentration of the compound and Hill indicates the Hill coefficient.

**Method for Determination of Activator Effects on Insulin Secretion in Dispersed Rat Islets.** Male Sprague–Dawley rats (200–275 g) were euthanized, and the pancreas was perfused via the common bile duct with ice cold Hank's balanced salt solution (HBSS, Gibco, No. 14185) containing 1.2 mM  $\text{CaCl}_2$ , 25 mM HEPES, 0.234 mg/mL liberase (Roche, No. 11815032001), and 0.07 mg/mL DNase (Sigma, No. D4527-200KU). The pancreas was removed and digested with stirring for 12 min at 37 °C on a submersible stir plate. Following digestion ice cold quench (HBSS, 10% FBS, 10 mM HEPES) was added and the pancreas was spun at 50g for 15 s. The supernatant was removed, and the pellet was resuspended in ice-cold quench and passed over a 250  $\mu$ m screen. The digested pancreas was again spun at 50g for 15 s, and the supernatant was removed. The pellet was resuspended in 8 mL of 27% Ficoll (Sigma, No. F9378) and transferred to a 30 mL Corex tube. An amount of 4 mL of 23% Ficoll was then layered in the tube followed by 4 mL of 20.5% Ficoll and 4 mL of 11% Ficoll. The sample was then spun at 500g for 10 min. The islets were removed from the upper layers of Ficoll and washed twice with HBSS without  $\text{Ca}^{2+}$ . Following washing, 1 mM EDTA was added and the islets were incubated for 8 min at room temperature. Next 0.00125% trypsin–EDTA and 2  $\mu$ g/mL DNase I (final concentrations) were added, and the islets were incubated for 10 min at 30 °C with shaking at 60 rpm. Following dispersion the islets were dissociated via 50 passes with a 1 mL pipet. The islets were diluted with culture medium (RPMI 1640, 10% FBS, L-glutamine, pen/strep, and HEPES) and passed over a 63  $\mu$ m nylon membrane. The dispersed islets were pelleted, then washed again with culture medium. After counting, the cells were suspended in culture medium and seeded at 5000 cells per well (200  $\mu$ L/well) in 96-well V bottom plates. The plates were spun for 5 min at 200g and then placed in a 5%  $\text{CO}_2$  cell culture incubator overnight.

Test articles were solubilized in 100% DMSO at 10 mM. Serial dilutions were made in 100% DMSO to 3, 1, 0.3, and 0.1 mM. The compound was further diluted in incubation buffer to final concentrations of 3, 1, 0.3, and 0.1  $\mu$ M.

The medium was aspirated from each well and replaced with 100  $\mu$ L of 3 mM glucose in incubation buffer (115 mM NaCl, 5 mM KCl, 24 mM  $\text{NaHCO}_3$ , 2.2 mM  $\text{CaCl}_2$ , 1 mM  $\text{MgCl}_2$ , 24 mM HEPES, 0.25% BSA). The dispersed islet plates were spun at 200g to repellet the islets and then incubated in a 37 °C water bath continuously gassed with 95%  $\text{O}_2$ /5%  $\text{CO}_2$  for 45 min. The preincubation buffer was then removed and replaced with 50  $\mu$ L of incubation buffer containing 3, 1, 0.3, and 0.1  $\mu$ M test article in 3, 5, 9, 11, 13, or 22 mM glucose, in replicates of 8. All glucose concentrations containing 0.1% DMSO were included on each plate as internal controls. The plates were spun to pellet the islets and then incubated for 60 min in a 37 °C water bath continuously gassed with 95%  $\text{O}_2$ /5%  $\text{CO}_2$ . Following the incubation an amount of 35  $\mu$ L of buffer was removed and transferred to a 96-well polypropylene storage plate and frozen. Insulin content was analyzed using a commercial EIA (Alpco, No. 80-INSRTH-E10). This

experiment was performed three times with three individual preparations of rat dispersed islets. Insulin secretion data were analyzed using GraphPad Prism. Data were normalized as % effect relative to maximum glucose, which in these studies was 22 mM. Data from the three individual experiments were averaged for graphing.

**Evaluation of the Effect Glucokinase Activators on Fasting and Postprandial Glucose in Goto–Kakizaki Rats.** Rats arrived at the facility at 7–8 weeks of age and were acclimated 1 week prior to test article/vehicle administration. Following a 1 week acclimation, rats were randomized by fed-state body weight into different treatment groups and dosed daily in the with vehicle (0.5% methylcellulose) or test article. Dosing was based on body weight at a concentration of 5 mL/kg and continued for 28 days. Blood samples (250  $\mu$ L) were collected in ethylenediaminetetraacetic acid (EDTA) treated microtainers, mixed by inversion, and placed on ice. Plasma was isolated via centrifugation at 14 000 rpm in an Eppendorf centrifuge 5417R at 4 °C for 2 min. The samples were then analyzed through the use of Roche Diagnostics clinical analyzer. Insulin levels were also measured using a diagnostics rat ultrasensitive insulin kit (Alpco). Rats underwent an end-study oral glucose tolerance test (OGTT) on day 28. Sixty minutes after test article administration, a blood sample was collected and the rats were immediately given a 2 g/kg oral bolus of 40% glucose in water. Subsequent blood samples were collected at 15, 30, 60, and 120 min after the oral glucose challenge.

## AUTHOR INFORMATION

### Corresponding Author

\*Phone: 617-551-3169. Fax: 617-551-3084. E-mail: jeffrey.a.pfefferkorn@pfizer.com.

## ABBREVIATIONS USED

CRR, counter-regulatory response; FPG, fasting plasma glucose; GK, glucokinase; GKA, glucokinase activator; GSIS, glucose-stimulated insulin secretion; HGP, hepatic glucose production; MODY, maturity onset diabetes of the young; OATP, organic anion transporting polypeptide; OGTT, oral glucose tolerance test; T2DM, type 2 diabetes mellitus

## REFERENCES

- (1) World Health Organization Diabetes Fact Sheet No. 312. <http://www.who.int/mediacentre/factsheets/fs312/en/> (accessed September 30, 2011).
- (2) Lebovitz, H. E. Management of Hyperglycemia with Oral Antihyperglycemic Agents in Type 2 Diabetes. In *Joslin's Diabetes Mellitus*, 14th ed.; Kahn, C. R., et al. Eds.; Lippincott Williams & Wilkins: Philadelphia, PA, 2005; pp 687–710.
- (3) For reviews, see the following: (a) Fyfe, M. C. T.; Procter, M. J. Glucokinase activators as potential antidiabetic drugs possessing superior glucose-lowering efficacy. *Drugs Future* **2009**, *34*, 641–653. (b) Matschinsky, F. Assessing the potential of glucokinase activators in diabetes therapy. *Nat. Rev. Drug Discovery* **2009**, *8*, 399–416.
- (4) Matschinsky, F.; Magnuson, M. A., Eds. *Glucokinase and Glycemic Diseases: From Basics to Novel Therapeutics*; Karger: Basel, Switzerland, 2004.
- (5) Matschinsky, F. M.; Glaser, B.; Magnuson, M. A. Pancreatic  $\beta$ -cell glucokinase: closing the gap between theoretical concepts and experimental realities. *Diabetes* **1998**, *47*, 307–315.
- (6) Heimberg, H.; De Vos, A.; Moens, K.; Quartier, E.; Bouwens, L.; Pipeleers, D.; Van Schaftingen, E.; Madsen, O.; Schuit, F. The glucose sensor protein glucokinase is expressed in glucagon-producing  $\alpha$ -cells. *Proc. Natl. Acad. Sci. U.S.A.* **1996**, *93*, 7036–7041.
- (7) (a) Agius, L. Glucokinase and molecular aspects of liver glycogen metabolism. *Biochem. J.* **2008**, *414*, 1–18. (b) Iynedjian, P. B. Molecular physiology of mammalian glucokinase. *Cell. Mol. Life Sci.* **2009**, *66*, 27–42.
- (8) Dunn-Meynell, A. A.; Routh, V. H.; Kang, L.; Gaspers, L.; Levin, B. E. Glucokinase is likely mediator of glucose sensing in both glucose-

excited and glucose-inhibited central neurons. *Diabetes* **2002**, *51*, 2056–2065.

(9) (a) Jetton, T. L.; Liang, Y.; Pettepher, C. C.; Zimmerman, E. C.; Cox, F. G.; Horvath, K.; Matschinsky, F. M.; Magnuson, M. A. Analysis of upstream glucokinase promoter activity in transgenic mice and identification of glucokinase in rare neuroendocrine cells in the brain and gut. *J. Biol. Chem.* **1994**, *269*, 3641–3654. (b) Murphy, R.; Tura, A.; Clark, P. M.; Holst, J. J.; Mari, A.; Hattersley, A. T. Glucokinase, the pancreatic glucose sensor, is not the gut glucose sensor. *Diabetologia* **2009**, *52*, 154–159.

(10) Zelent, D.; Golson, M. L.; Koeberlein, B.; Quintens, R.; van Lommel, L.; Buettger, C.; Weik-Collins, H.; Taub, R.; Grimsby, J.; Schuit, F.; Kaestner, K. H.; Matschinsky, F. M. A glucose sensor role for glucokinase in anterior pituitary cells. *Diabetes* **2006**, *55*, 1923–1929.

(11) For a review, see the following: Gloyn, A. L. Glucokinase (GCK) mutations in hyper- and hypoglycemia: maturity-onset diabetes of the young, permanent neonatal diabetes, and hyperinsulinemia of infancy. *Hum. Mutat.* **2003**, *22*, 353–362.

(12) Grimsby, J.; Sarabu, R.; Corbett, W. L.; Haynes, N. E.; Bizzarro, F. T.; Coffey, J. W.; Guertin, K. R.; Hilliard, D. W.; Kester, R. F.; Mahaney, P. E.; Marcus, L.; Qi, L.; Spence, C. L.; Teng, J.; Magnuson, M. A.; Chu, C. A.; Dvorozniak, M. T.; Matschinsky, F. M.; Grippo, J. F. Allosteric activators of glucokinase: potential role in diabetes therapy. *Science* **2003**, *301*, 370–373.

(13) Haynes, N. E.; Corbett, W. L.; Bizzarro, F. T.; Guertin, K. R.; Hilliard, D. W.; Holland, G. W.; Kester, R. F.; Mahaney, P. E.; Qi, L.; Spence, C. L.; Teng, J.; Dvorozniak, M. T.; Railkar, A.; Matschinsky, F. M.; Grippo, J. F.; Grimsby, J.; Sarabu, R. Discovery, structure–activity relationships, pharmacokinetics, and efficacy of glucokinase activator (2R)-3-cyclopentyl-2-(4-methanesulfonylphenyl)-N-thiazol-2-yl-propionamide (RO0281675). *J. Med. Chem.* **2010**, *53*, 3618–3625.

(14) (a) Kester, R. F.; Corbett, W. L.; Sarabu, R.; Mahaney, P. E.; Haynes, N. E.; Guertin, K. R.; Bizzarro, F. T.; Hilliard, D. W.; Qi, L.; Teng, J.; Grippo, J. F.; Grimsby, J.; Marcus, L.; Spence, C.; Dvorozniak, M.; Racha, J.; Wang, K. Discovery of Piragliatin, a Small Molecule Activator of GK. Presented at the 238th National Meeting of the American Chemical Society, Washington, DC, August 16–20, 2009; MEDI-005. (b) Sarabu, R.; Tilley, J. W.; Grimsby, J. The discovery of piragliatin, a glucokinase activator. *RSC Drug Discovery Ser.* **2011**, *4*, 51–70.

(15) Bertram, L. S.; Black, D.; Briner, P. H.; Chatfield, R.; Cooke, A.; Fyfe, M. C. T.; Murray, P. J.; Naud, F.; Nawano, M.; Procter, M. J.; Rakipovski, G.; Rasamison, C. M.; Reynet, C.; Schofield, K. L.; Shah, V. K.; Spindler, F.; Taylor, A.; Turton, R.; Williams, G. M.; Wong-Kai-In, P.; Yasuda, K. SAR, pharmacokinetics, safety, and efficacy of glucokinase activating 2-(4-sulfonylphenyl)-N-thiazol-2-ylacetamides: discovery of PSN-GK1. *J. Med. Chem.* **2008**, *51*, 4340–4345.

(16) Beberitz, G. R.; Beaulieu, V.; Dale, B. A.; Deacon, R.; Duttaroy, A.; Gao, J.; Grondine, M. S.; Gupta, R. C.; Kakmak, M.; Kavana, M.; Kirman, L. C.; Liang, J.; Maniara, W. M.; Munshi, S.; Nadkarni, S. S.; Schuster, H. F.; Stams, T.; Denny, I. S.; Taslimi, P. M.; Vash, B.; Caplan, S. L. Investigation of functionally liver selective glucokinase activators for the treatment of type 2 diabetes. *J. Med. Chem.* **2009**, *52*, 6142–6152.

(17) Kamata, K.; Mitsuya, M.; Nishimura, T.; Eiki, J.; Nagata, Y. Structural basis for allosteric regulation of the monomeric allosteric enzyme human glucokinase. *Structure* **2004**, *12*, 429–438.

(18) Waring, M. J.; Johnstone, C.; McKerrecher, D.; Pike, K. G.; Robb, G. Matrix-based multiparameter optimization of glucokinase activators: the discovery of AZD1092. *Med. Chem. Commun.* **2011**, *2*, 775–779.

(19) Klapars, A.; Campos, C. R.; Waldman, J. H.; Zewge, D.; Dormer, P. G.; Chen, C.-Y. Enantioselective Pd-catalyzed  $\alpha$ -arylation of N-Boc-pyrrolidine: the key to an efficient and practical synthesis of a glucokinase activator. *J. Org. Chem.* **2008**, *73*, 4986–4993.

(20) Yoshikawa, N.; Xu, F.; Arredondo, J. D.; Itoh, T. A large-scale synthesis of potent glucokinase activator MK-0941 via selective O-arylation and O-alkylation. *Org. Process Res. Dev.* **2011**, *15*, 824–830.

(21) Pike, K. G.; Allen, J. V.; Caulkett, P. W.; Clarke, D. S.; Donald, C. S.; Fenwick, M. L.; Johnson, K. M.; Johnstone, C.; McKerrecher, D.; Rayner, J. W.; Walker, R. P.; Wilson, I. Design of a potent, soluble glucokinase activator with increased pharmacokinetic half-life. *Bioorg. Med. Chem. Lett.* **2011**, *21*, 3467–3470.

(22) For recent reviews of glucokinase activators, see the following: (a) Coghlan, M.; Leighton, B. Glucokinase activators in diabetes management. *Expert Opin. Invest. Drugs* **2008**, *17*, 145–167. (b) Sarabu, R.; Berthel, S. J.; Kester, R. F.; Tilley, J. W. Glucokinase activators as new type 2 diabetes therapeutic agents. *Expert Opin. Ther. Pat.* **2008**, *18*, 759–768. (c) Sarabu, R.; Berthel, S. J.; Kester, R. F.; Tilley, J. W. Novel glucokinase activators: a patent review (2008–2010). *Expert Opin. Ther. Patents* **2011**, *21*, 13–31.

(23) For reports of glucokinase activator clinical efficacy and safety, see the following: (a) Zhi, J.; Zhai, S.; Mulligan, M.-E.; Grimsby, J.; Arbet-Engels, C.; Boldrin, M.; Balena, R. A novel glucokinase activator RO4389620 improved fasting and postprandial glucose in type 2 diabetic patients. *Diabetologia* **2008**, *51* (Suppl. 1), S23, Abstract 42. (b) Zhai, S.; Mulligan, M.-E.; Grimsby, J.; Arbet-Engels, C.; Boldrin, M.; Balena, R.; Zhi, J. Phase 1 assessment of a novel glucokinase activator RO4389620 in healthy male volunteers. *Diabetologia* **2008**, *51* (Suppl. 1), S372, Abstract 928. (c) Bonadonna, R. C.; Heise, T.; Arbet-Engels, C.; Kapitza, C.; Avogaro, A.; Grimsby, J.; Zhi, J.; Grippo, J. F.; Balena, R. Piragliatin (RO4389620), a novel glucokinase activator, lowers plasma glucose both in the postabsorptive state and after a glucose challenge in patients with type 2 diabetes mellitus: a mechanistic study. *J. Clin. Endocrinol. Metab.* **2010**, *95*, 5028–5036. (d) Migoya, E.; Miller, J.; Moreau, M.; Reitman, C.; Maganti, L.; Larson, P.; Gutierrez, M.; Morrow, L.; Denoia, E.; Gottesdiener, K.; Wagner, J. A. Additional Glucose-Lowering Effects of Oral GK Activator, MK-0941, in Patients with T2DM on Basal Insulin. Presented at the 71st American Diabetes Association Meeting, San Diego, CA, 2011. (e) Bue-Valleskey, J. M.; Schneck, K. B.; Sinha, V. P.; Wondmagegnehu, E. T.; Kapitza, C.; Miller, J. W. LY2599506, a Novel Glucokinase Activator (GKA), Improves Fasting and Postprandial Glucose in Patients with Type 2 Diabetes Mellitus (T2DM). Presented at the 71st American Diabetes Association Meeting, San Diego, CA, 2011.

(24) Pfefferkorn, J. A.; Guzman-Perez, A.; Oates, P. J.; Litchfield, J.; Aspnes, G.; Basak, A.; Benbow, J.; Berliner, M. A.; Bian, J.; Choi, C.; Freeman-Cook, K.; Corbett, J. W.; Didiuk, M.; Dunetz, J. R.; Filipski, K. J.; Hungerford, W. M.; Jones, C. S.; Karki, K.; Ling, A.; Li, J.-C.; Patel, L.; Perreault, C.; Risley, H.; Saenz, J.; Song, W.; Tu, M.; Aiello, R.; Atkinson, K.; Barucci, N.; Beebe, D.; Bourassa, P.; Bourbounais, F.; Brodeur, A. M.; Burbey, R.; Chen, J.; D'Aquila, T.; Derksen, D. R.; Haddish-Berhane, N.; Huang, C.; Landro, J.; Lee Lapworth, A.; MacDougall, M.; Perregaux, D.; Pettersen, J.; Robertson, A.; Tan, B.; Treadway, J. L.; Liu, S.; Qiu, X.; Knafels, J.; Ammirati, M.; Song, X.; DaSilva-Jardine, P.; Liras, S.; Sweet, L.; Rolph, T. P. Designing glucokinase activators with reduced hypoglycemia risk: discovery of N,N-dimethyl-5-(2-methyl-6-((5-methylpyrazin-2-yl)-carbamoyl)-benzofuran-4-yloxy)pyrimidine-2-carboxamide as a clinical candidate for the treatment of type 2 diabetes mellitus. *Med. Chem. Commun.* **2011**, *2*, 828–839.

(25) Bödvarsdóttir, T. B.; Wahl, P.; Santhosh, K. C.; Polisetti, D. R.; Guzel, M.; Fosgerau, Larsen, M. Ø.; Halberg, I. B.; Selmer, J.; Andrews, R. C.; Mjalli, A. M. M.; Valcarce, V. TTP355, a Glucokinase Activator. Presented at the 68th American Diabetes Association Meeting, San Francisco, CA, 2008.

(26) Caro, J. F.; Triester, S.; Patel, V. K.; Tapscott, E. B.; Frazier, N. L.; Dohm, G. L. Liver glucokinase: decreased activity in patients with type II diabetes. *Horm. Metab. Res.* **1995**, *27*, 19–22.

(27) Basu, A.; Basu, R.; Shah, P.; Vella, A.; Johnson, C. M.; Nair, K. S.; Jensen, M. D.; Schwenk, W. F.; Rizza, R. A. Effects of type 2 diabetes on the ability of insulin and glucose to regulate splanchnic and



muscle glucose metabolism. Evidence for a defect in hepatic glucokinase activity. *Diabetes* **2000**, *49*, 272–283.

(28) For an example, see the following: Torres, T. P.; Catlin, R. L.; Chan, R.; Fujimoto, Y.; Sasaki, N.; Printz, R. L.; Newgard, C. B.; Shiota, M. Restoration of hepatic glucokinase expression corrects hepatic glucose flux and normalizes plasma glucose in Zucker diabetic fatty rats. *Diabetes* **2009**, *58*, 78–86.

(29) (a) Pfefferkorn, J. A.; Litchfield, J.; Hutchings, R.; Cheng, X.-M.; Larsen, S. D.; Auerbach, B.; Bush, M. R.; Lee, C.; Erasga, N.; Bowles, D. M.; Boyles, D. C.; Lu, G.; Sekerke, C.; Askew, V.; Hanselman, J. C.; Dillon, L.; Lin, Z.; Robertson, A.; Olsen, K.; Boustany, C.; Atkinson, K.; Goosen, T. C.; Sahasrabudhe, V.; Chupka, J.; Duignan, D. B.; Feng, B.; Scialis, R.; Kimoto, E.; Bi, Y.-A.; Lai, Y.; El-Kattan, A.; Bakker-Arkema, R.; Barclay, P.; Kindt, E.; Le, V.; Mandema, J. W.; Milad, M.; Tait, B. D.; Kennedy, R.; Trivedi, B. K.; Kowala, M. Discovery of novel hepatoselective HMG-CoA reductase inhibitors for treating hypercholesterolemia: a bench-to-bedside case study on tissue selective drug distribution. *Bioorg. Med. Chem. Lett.* **2011**, *21*, 2725–2731. (b) Ahmad, S.; Madsen, C. S.; Stein, P. D.; Janovitz, E.; Huang, C.; Ngu, K.; Bisaha, S.; Kennedy, L. J.; Chen, B. C.; Zhao, R.; Sitkoff, D.; Monshizadegan, H.; Yin, X.; Ryan, C. S.; Zhang, R.; Giancarli, M.; Bird, E.; Chang, M.; Chen, X.; Setters, R.; Search, D.; Zhuang, S.; Nguyen-Tran, V.; Cuff, C. A.; Harrity, T.; Darienzo, C. J.; Li, T.; Reeves, R. A.; Blamar, M. A.; Barrish, J. C.; Zahler, R.; Robl, J. A. (3*R*,5*S*,*E*)-7-(4-(4-fluorophenyl)-6-isopropyl-2-(methyl(1-methyl-1*H*-1,2,4-triazol-5-yl)amino)pyrimidin-5-yl)-3,5-dihydroxyhept-6-enoic acid (BMS-644950): a rationally designed orally efficacious 3-hydroxy-3-methylglutaryl coenzyme-A reductase inhibitor with reduced myotoxicity potential. *J. Med. Chem.* **2008**, *51*, 2722–2733. (c) Pfefferkorn, J. A.; Choi, C.; Larsen, S. D.; Auerbach, B.; Hutchings, R.; Park, W.; Askew, V.; Dillon, L.; Hanselman, J. C.; Lin, Z.; Lu, G. H.; Robertson, A.; Sekerke, C.; Harris, M. S.; Pavlovsky, A.; Bainbridge, G.; Caspers, N.; Kowala, M.; Tait, B. D. Substituted pyrazoles as hepatoselective HMG-CoA reductase inhibitors: discovery of (3*R*,5*R*)-7-[2-(4-fluoro-phenyl)-4-isopropyl-5-(4-methyl-benzylcarbamoyl)-2*H*-pyrazol-3-yl]-3,5-dihydroxyheptanoic acid (PF-3052334) as a candidate for the treatment of hypercholesterolemia. *J. Med. Chem.* **2008**, *51*, 31–45.

(30) (a) Oballa, R. M.; Belair, L.; Black, W. C.; Bleasby, K.; Chan, C. C.; Desroches, C.; Du, X.; Gordon, R.; Guay, J.; Guiral, S.; Hafey, M. J.; Hamelin, E.; Huang, Z.; Kennedy, B.; Lachance, N.; Landry, F.; Li, C. S.; Mancini, J.; Normandin, D.; Poci, A.; Powell, D. A.; Ramtohl, Y. K.; Skorey, K.; Sorensen, D.; Sturkenboom, W.; Styhler, A.; Waddleton, D. M.; Wang, H.; Wong, S.; Xu, L.; Zhang, L. Development of a liver-targeted stearoyl-CoA desaturase (SCD) inhibitor (MK-8245) to establish a therapeutic window for the treatment of diabetes and dyslipidemia. *J. Med. Chem.* **2011**, *54*, 5082–5096. (b) Koltun, D. O.; Zilbershtein, T. M.; Migulin, V. A.; Vasilevich, N. I.; Parkhill, E. Q.; Glushkov, A. I.; McGregor, M. J.; Brun, S. A.; Chu, N.; Hao, J.; Mollova, N.; Leung, K.; Chisholm, J. W.; Zablocki, J. Potent, orally bioavailable, liver-selective stearoyl-CoA desaturase (SCD) inhibitors. *Bioorg. Med. Chem. Lett.* **2009**, *19*, 4070–4074. (c) Leclerc, J.-P.; Falgout, J.-P.; Girardin, M.; Guay, J.; Guiral, S.; Huang, Z.; Li, C. S.; Oballa, R.; Ramtohl, Y. K.; Skorey, K.; Tawa, P.; Wang, H.; Zhang, L. Conversion of systemically distributed triazole-based stearoyl-CoA desaturase (SCD) uHTS hits into liver-targeted SCD inhibitors. *Bioorg. Med. Chem. Lett.* **2011**, *21*, 6505–6509.

(31) (a) von Geldern, T. W.; Tu, N.; Kym, P. R.; Link, J. T.; Jae, H.-S.; Lai, C.; Apelqvist, T.; Rhonstad, P.; Hagberg, L.; Koehler, K.; Grynfarb, M.; Goos-Nilsson, A.; Sandberg, J.; Österlund, M.; Barkhem, T.; Höglund, M.; Wang, J.; Fung, S.; Wilcox, D.; Nguyen, P.; Jakob, C.; Hutchins, C.; Färnegårdh, M.; Kauppi, B.; Öhman, L.; Jacobson, P. B. Liver-selective glucocorticoid antagonists: a novel treatment for type 2 diabetes. *J. Med. Chem.* **2004**, *47*, 4213–4230. (b) Link, J. T.; Sorensen, B. K.; Lai, C.; Wang, J.; Fung, S.; Deng, D.; Emery, M.; Carroll, S.; Grynfarb, M.; Goos-Nilsson, A.; von Geldern, T. Synthesis, activity, metabolic stability, and pharmacokinetics of glucocorticoid

receptor modulator–statin hybrids. *Bioorg. Med. Chem. Lett.* **2004**, *14*, 4173–4178.

(32) Boyer, S. H.; Jiang, H.; Jacintho, J. D.; Reddy, M. V.; Li, H.; Godwin, J. L.; Schulz, W. G.; Cable, E. E.; Hou, J.; Wu, R.; Fujitaki, J. M.; Hecker, S. J.; Erion, M. D. Synthesis and biological evaluation of a series of liver-selective phosphonic acid thyroid hormone receptor agonists and their prodrugs. *J. Med. Chem.* **2008**, *51*, 7075–7093.

(33) For a review, see the following: Erion, M. D.; Bullough, D. A.; Lin, C.-C.; Hong, Z. HepDirect prodrugs for targeting nucleotide-based antiviral drugs to the liver. *Curr. Opin. Invest. Drugs* **2006**, *7*, 109–117.

(34) Hoglen, N. C.; Chen, L.-S.; Fisher, C. D.; Hirakawa, B. P.; Groessl, T.; Contreras, P. C. Characterization of IDN-6556 (3-{2-(2-*tert*-butyl-phenylaminoxy)-amino}-propionylamino}-4-oxo-5-(2,3,5,6-tetrafluoro-phenoxy)-pentanoic acid): a liver-targeted caspase inhibitor. *J. Pharmacol. Exp. Ther.* **2004**, *309*, 634–640.

(35) Boyer, S. H.; Sun, Z.; Jiang, H.; Esterbrook, J.; Gómez-Galeno, J. E.; Craig, W.; Reddy, K. R.; Ugarkar, B. G.; MacKenna, D. A.; Erion, M. D. Synthesis and characterization of a novel cyclic 1-aryl-1,3-propanyl prodrug of cytarabine monophosphate (MB07133) for the treatment of hepatocellular carcinoma. *J. Med. Chem.* **2006**, *49*, 7711–7720.

(36) Brocklehurst, K. J.; Payne, V. A.; Davies, R. A.; Carroll, D.; Vertigan, H. L.; Wightman, H. J.; Aiston, S.; Waddell, I. D.; Leighton, B.; Coghlan, M. P.; Agius, L. Stimulation of hepatocyte glucose metabolism by novel small molecule glucokinase activators. *Diabetes* **2004**, *53*, 535–541.

(37) Segel, I. H. *Enzyme Kinetics: Behavior and Analysis of Rapid Equilibrium and Steady State Enzyme Systems*; Wiley: New York, 1993.

(38) Kalgutkar, A. S.; Feng, B.; Nguyen, H. T.; Frederick, K. S.; Campbell, S. D.; Hatch, H. L.; Bi, Y. A.; Kazolias, D. C.; Davidson, R. E.; Mireles, R. J.; Duignan, D. B.; Choo, E. F.; Zhao, S. X. Role of transporters in the disposition of the selective phosphodiesterase-4 inhibitor (+)-2-[4-({2-(benzo[1,3]dioxol-5-yloxy)-pyridine-3-carbonyl}-amino)-methyl]-3-fluoro-phenoxy]-propionic acid in rat and human. *Drug Metab. Dispos.* **2007**, *35*, 2111–2118.

(39) Di, L.; Whitney-Pickett, C.; Umland, J. P.; Zhang, H.; Zhang, X.; Gebhard, D. F.; Lai, Y.; Federico, J. J.; Davidson, R. E.; Smith, R.; Reyner, E. L.; Lee, C.; Feng, B.; Rotter, C.; Varma, M. V.; Kempshall, S.; Fenner, K.; El-Kattan, A. F.; Liston, T. E.; Troutman, M. D. Development of a new permeability assay using low-efflux MDCKII cells. *J. Pharm. Sci.* **2011**, *100*, 4974–4985.

(40) (a) Cryle, M. J.; Matovic, N. J.; De Voss, J. J. Products of cytochrome P450BioI (CYP107H1)-catalyzed oxidation of fatty acids. *Org. Lett.* **2003**, *5*, 3341–3344. (b) Larcheveque, M.; Petit, Y. A simple preparation of *R* or *S* glycidic esters; application to the synthesis of enantiomerically pure  $\alpha$ -hydroxyesters. *Tetrahedron Lett.* **1987**, *28*, 1993–1996.

(41) Pfefferkorn, J. A.; Lou, J.; Minich, M. L.; Filipinski, K. J.; He, M.; Zhou, R.; Ahmed, S.; Benbow, J.; Guzman-Perez, A.; Tu, M.; Litchfield, J.; Sharma, R.; Metzler, K.; Bourbonais, F.; Huang, C.; Beebe, D.; Oates, P. J. Pyridones as glucokinase activators: identification of a unique metabolic liability of the 4-sulfonyl-2-pyridone heterocycle. *Bioorg. Med. Chem. Lett.* **2009**, *19*, 3247–3252.

(42) For other representative examples where structure-based strategies have utilized solvent exposed pockets to modulate molecular properties, see the following: (a) Sun, L.; Liang, C.; Shirazian, S.; Zhou, Y.; Miller, T.; Cui, J.; Fukuda, J. Y.; Chu, J.-Y.; Nematala, A.; Wang, X.; Chen, H.; Sistla, A.; Luu, T. C.; Tang, F.; Wei, J.; Tang, C. Discovery of 5-[5-fluoro-2-oxo-1,2-dihydroindol-(3*Z*)-ylidenemethyl]-2,4-dimethyl-1*H*-pyrrole-3-carboxylic acid (2-diethylaminoethyl)amide, a novel tyrosine kinase inhibitor targeting vascular endothelial and platelet-derived growth factor receptor tyrosine kinase. *J. Med. Chem.* **2003**, *46*, 1116–1119. (b) Plantan, I.; Selic, L.; Mesar, T.; Stefanic Anderluh, P.; Oblak, M.; Prezelj, A.; Hesse, L.; Andrejasic, M.; Vilar, M.; Turk, D.; Kocijan, A.; Prevec, T.; Vilfan, G.; Kocijan, D.; Copar, A.; Urleb, U.; Solmajer, T. 4-Substituted trinemins as broad spectrum  $\beta$ -lactamase inhibitors: structure-based

design, synthesis, and biological activity. *J. Med. Chem.* **2007**, *50*, 4113–4121.

(43) For more detailed account of the steady state kinetic interaction of **19** with the glucokinase enzyme, see the following: Bourbonais, F. J.; Chen, J.; Huang, C.; Zhang, Y.; Pfefferkorn, J. A.; Landro, J. A. Modulation of glucokinase by glucose, small molecule activator and glucokinase regulatory protein: steady-state kinetic and cell-based analysis. *Biochem. J.* [Online early access]. DOI: 10.1042/BJ20110721. Published Online: Nov 1, **2011**.

(44) Barucci, N.; Robertson, A. S.; Bourassa, P.; Baker, L.; Mather, D.; Perregaux, D. G.; Treadway, J. L.; Walton, J.; Atkinson, K.; Hellembaek, J.; Tan, B.; Pfefferkorn, J. A.; Boustany, C.; D'Aquila, T.; Litchfield, J.; Aiello, R. Characterization of a Potent Glucokinase Activator with Diminished Risk of Hypoglycemia. Presented at the 71st American Diabetes Association Meeting, San Diego, CA, 2011.

(45) Previous reports have found that cryopreservation and culture conditions can significantly affect transporter expression in rat hepatocytes. For example, see the following: Jørgensen, L.; Van Beek, J.; Lund, S.; Schousboe, A.; Badolo, L. Evidence of Oatp and Mdr1 in cryopreserved rat hepatocytes. *Eur. J. Pharm. Sci.* **2007**, *30*, 181–189. This should be considered during potency comparisons between actively and nonactively transported compounds and when interpreting absolute potencies in these systems.

(46) Pettersen, J.; Litchfield, J.; Neef, N.; Schmidt, S. P.; Shirai, N.; Walters, K.; Enerson, B.; Pfefferkorn, J. The Relationship of Glucokinase Activator Induced Hypoglycemia with Cardiac Arterio-pathy, Neuronal Necrosis and Peripheral Neuropathy in Nonclinical Toxicology Studies. Presented at the 50th Annual Meeting of the Society of Toxicology, Washington, DC, March 6–10, 2011.

(47) Loxham, S. J. G.; Teague, J.; Poucher, S. M.; Schoolmeester, J. D.; Turnbull, A. V.; Carey, F. Glucagon challenge in the rat: a robust method for the in vivo assessment of glycogen phosphorylase inhibitor efficacy. *J. Pharmacol. Toxicol. Methods* **2007**, *55*, 71–77.

(48) (a) Unger, R. H.; Orci, L. Role of glucagon in diabetes. *Arch. Intern. Med.* **1977**, *137*, 482–491. (b) Dunning, B. E.; Gerich, J. E. The role of  $\alpha$ -cell dysregulation in fasting and postprandial hyperglycemia in type 2 diabetes and therapeutic implications. *Endocr. Rev.* **2007**, *28*, 253–283.

(49) Wachi, K.; Terada, A. Studies of 1,3-benzoxazines. I. Synthesis of primary 2-aminopyridines via the reaction of imidoyl chlorides of 1,3-benzoxazines with pyridine *N*-oxides. *Chem. Pharm. Bull.* **1980**, *28*, 465–472.

(50) Bessmertnykh, A.; Douaihy, C. M.; Muniappan, S.; Guillard, R. Efficient palladium-catalyzed synthesis of aminopyridyl phosphonates from bromopyridines and diethyl phosphite. *Synthesis* **2008**, 1575–1579.

(51) Holland, G. F.; Pereira, J. N. Heterocyclic tetrazoles, a new class of lipolysis inhibitors. *J. Med. Chem.* **1967**, *10*, 149–154.